SPECIAL PUBLICATIONS

SHIVA STRUCTURE: A POSSIBLE KT BOUNDARY IMPACT CRATER ON THE WESTERN SHELF OF INDIA

SANKAR CHATTERJEE, NECIP GUVEN, AARON YOSHINOBU,
AND RICHARD DONOFRIO

Front cover: Cover illustration showing the three-dimensional reconstruction of the submerged Shiva crater (~500 km diameter) at the Mumbai Offshore Basin, western shelf of India from different cross-sectional and geophysical data. The overlying 7-km-thick Cenozoic strata and water column were removed to show the morphology of the crater.

SPECIAL PUBLICATIONS

Museum of Texas Tech University

Number 50

Shiva Structure: A Possible KT Boundary Impact Crater on the Western Shelf of India

SANKAR CHATTERJEE, NECIP GUVEN, AARON YOSHINOBU, AND RICHARD DONOFRIO

Shiva Structure: A Possible KT Boundary Impact Crater on the Western Shelf of India

Sankar Chatterjee, Necip Guven, Aaron Yoshinobu, and Richard Donofrio

Abstract

Evidence is accumulating for multiple impacts across the Cretaceous-Tertiary (KT) transition, such as the Chicxulub crater in Yucatan Peninsula, Mexico, the Shiva crater offshore western India, and the much smaller Boltysh crater in Ukraine. Among these, the submerged Shiva crater on the Mumbai Offshore Basin on the western shelf of India is the largest (~500 km diameter), which is covered by 7-km-thick strata of Cenozoic sediments. It is a complex peak ring crater with a multiring basin, showing a structural relief of 7 km. A ring of peak is surrounded by an annular trough, which is bounded by a collapsed outer rim. Four different ring structures have been identified: an inner ring (peak ring) with a diameter of 200 km, a second 250-km-ring, a third ring (final crater rim) of about 500 km, and a probable exterior elevated ring of about 550 km. The crater outline is irregular squarish with a tapering end to the northeast indicating a possible oblique impact in a SW-NE direction. We speculate that the Shiva bolide (~40 km diameter) crashed obliquely on the western continental shelf of India around 65 Ma, excavating the crater and shattering the lithosphere. The peak ring of the Bombay High area has a core of Neoproterozoic granite with a veneer of Deccan Trap that rebounded upward for more than 50 km during the transient cavity stage as revealed by the mantle upwarping. Pseudotachylite veins of silica melt are observed within the drill cores of granitic target rock that may be linked to the impact-melting event. The combined Neoproterozoic granite and Deccan Trap target lithologies generated two kinds of impact melt ejecta that were emplaced radially in the downrange direction within the Deccan lava pile: rhyolite dikes, and iridium-rich alkaline igneous complexes. The age of the crater is inferred from its brecciated Deccan lava floor and the overlying Paleocene Panna Formation within the basin, isotopic dating of the presumed proximal ejecta melts, and the magnetic anomaly of the Carlsberg Ridge that was created by the impact. Concentric geophysical anomalies, thermal anomalies, seismic reflection, and structural and drill core data endorse the impact origin of the Shiva structure. The KT boundary sections in India, often preserved within the Deccan lava flows, have yielded several cosmic signatures of impact such as an iridium anomaly, iridium-rich alkaline melt rocks, shocked quartz, nickel-rich spinels, magnetic and superparamagnetic iron particles, nickel-rich vesicular glass, sanidine spherules, high-pressure fullerenes, glass-altered smectites, and possibly impact-generated tsunami deposits. The impact was so intense that it led to several geodynamic anomalies: it fragmented, sheared, and deformed the lithospheric mantle across the western Indian margin and contributed to major plate reorganization in the Indian Ocean. This resulted in a 500-km displacement of the Carlsberg Ridge and initiated rifting between India and the Seychelles. At the same time, the spreading center of the Laxmi Ridge jumped 500 km westerly close to the Carlsberg Ridge. The oblique impact may have generated spreading asymmetry, which caused the sudden northward acceleration of the Indian plate in Early Tertiary. The central uplift of a complex crater and the shattered basement rocks and overlying sedimentary layers form an ideal structural trap for oil and gas. Many of the complex impact structures and events at the KT transition such as the Shiva crater, Chicxulub crater, and the Boltysh crater create the most productive hydrocarbon sites on the planet. The kill mechanisms associated with the Shiva impact appears to be sufficiently powerful to cause worldwide collapse of the climate and ecosystems leading to the KT mass extinction when the dinosaurs and two-thirds of all marine animal species were wiped out.

Key words: Cretaceous-Tertiary boundary, Deccan Traps, dinosaur extinction, India, Shiva crater

INTRODUCTION

Mass extinctions in Earth's history are generally attributed to bolide impacts or major flood basalt volcanism that had devastating effects on environment and climate leading to biotic crisis (Glen 1990, 1994). Even though Earth has clear evidence of a long history of extraterrestrial impact events, only the Cretaceous-Tertiary (KT) boundary impact has been studied well enough to find a causal connection between impact and mass extinction. The initial discovery of anomalous iridium (Alvarez et al. 1980), glass spherules (Smit 1999; Smit and Klaver 1981), and shocked quartz (Bohor 1990; Bohor et al. 1984) at the KT boundary sections in many parts of the world was interpreted as the evidence for a large bolide impact. The impact theory was bolstered with the discovery of the Chicxulub crater buried beneath the shore of the Yucatan Peninsula, Mexico. Chicxulub measures about 180-300 km in diameter and matches the predicted size and age of the long-sought KT impact site (Hilderbrand et al. 1991, 1995). It has been dubbed "the smoking gun" for the KT impact event that caused the catastrophic biotic crisis. Subsequent work including geochemistry (Blum et al. 1993), radiometric age of the melt rock from the Chicxulub crater (Swisher et al. 1992), impact ejecta layers (Smit 1999), and tsunami deposits (Bourgeois et al. 1988) at several KT boundary sections around the Gulf of Mexico lend further support to the hypothesis that Chicxulub does indeed mark ground zero for a colossal bolide impact at 65 Ma.

However, Keller et al. (2003, 2004) have accumulated a large body of evidence from well data within the Chicxulub crater indicating that this crater predates the KT boundary. They suggest that the crater was formed 300,000 years before the KT boundary and was much smaller (<120 km diameter) than originally hypothesized. These authors argue that there are several other craters of the appropriate age including the 24-km-wide Boltysh crater of Ukraine (Kelley and Gurov 2002), 20-km-wide Silverpit crater of the North Sea (Stewart and Allen 2002), and the gigantic Shiva crater of India (Chatterjee and Rudra 1996) that may support a multiple impact hypothesis for the KT mass extinction (Fig. 1). In this view, the KT mass extinction was caused not by a single bolide, but by a barrage of them (Chatterjee 1997). Doubt has been cast recently on the interpretation of the impact origin of the Silverpit crater, when it was reported that Silverpit might be a sinkhole basin caused by salt withdrawl resulting in a concentric array of normal faults (Underhill 2004).

The Shiva crater, located on the western continental margin of India around the Bombay High area, has emerged as a viable candidate for the KT impact site (Chatterjee 1992, 1997; Chatterjee and Rudra 1996; Chatterjee et al. 2003). Straddling the western coastline of India and almost entirely below water, the Shiva structure is located on the Mumbai Offshore Basin (MOB) and is buried by 7-km thick strata of post-impact Tertiary sediments. It has the morphology of a complex crater, with a series of central structural uplifts in the form of a peak ring, an annular trough, and a collapsed outer rim. If confirmed as an impact site, the Shiva crater would be the largest impact crater known on Earth, about 500 km in diameter. The purpose of this paper is to integrate available geological, geophysical, geochemical data on the Shiva structure and to examine its likely impact origin at KT boundary.

LOCATION OF THE SHIVA CRATER

The exact location and size of the Shiva structure are controversial because it is largely submerged and buried by thick sediments on the western shelf of India, as well as by thick Deccan lava piles on its eastern margin. Thus, it is inaccessible for direct study. Moreover, the close spatial and temporal coincidence of the Shiva crater with the India-Seychelles rifting event and the widespread Deccan volcanism make it
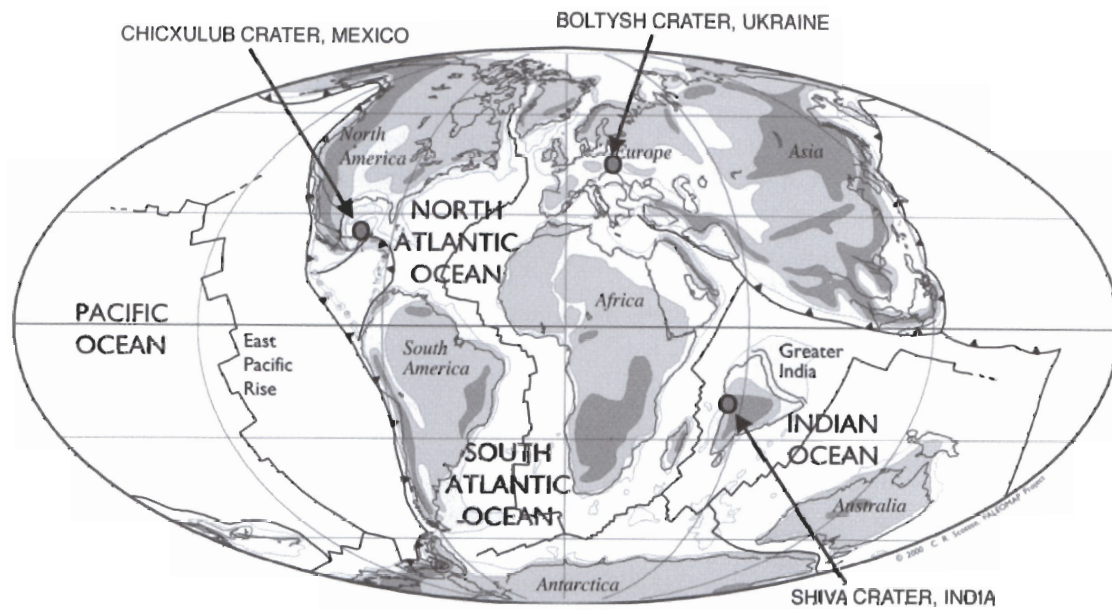
Figure 1. Positions of the continents at Cretaceous-Tertiary (KT) transition around 65 Ma, when multiple impact craters were formed: the Chicxulub crater in Mexico is about 180 km diameter, the Boltysh crater in Ukraine is about 25 km diameter, whereas the Shiva crater in India is about 500 km diameter (modified from Scotese 1997). Recent work suggests that the Chicxulub crater may be 300,000 years older than the KT boundary and might not be directly involved with the KT mass extinction (Keller et al. 2003). All these craters are excellent structural traps for giant oil and gas fields.

more difficult to delineate the size and location of the crater.

Hartnady (1986) and Alt et al. (1988) proposed that the subcircular Amirante Ridge and its enclosed basin southwest of Seychelles, might be the western rim of a possible impact crater, but its eastern rim lies along the western coast of India, hidden by the overlying Deccan Traps. They proposed that the force of the impact was so powerful that it could have cracked the lithosphere, such that the Deccan Traps represent impact-related melts that filled the crater to form an immense lava lake, the terrestrial equivalent of a lunar mare.

Chatterjee and Rudra (1996) elaborated upon this impact site at the India-Seychelles rift margin, and identified the eastern half of the crater at the Mumbai Offshore Basin (MOB), where the crater is bounded by the Panvel Flexure near the Mumbai coast and the Narmada Fault in the western Arabian Sea. They reconstructed the size and shape of the impact structure by incorporating the Amirante arc and named it Shiva crater after the Hindu god of destruction. They proposed that the Carlsberg rifting, which might be triggered by the impact itself, splits the Shiva crater into halves and separated India from the Seychelles. Today, one part of the crater is attached to the Seychelles, and the other part is attached to the western coast of India.

Chatterjee and Rudra (1996) argued that if the Amirante Basin were indeed the western rim of the Shiva crater, the Mahe granite on the Seychelles, which superficially looks like a shattered and chaotic assemblage of gigantic blocks (Baker 1967), should bear some sign of an impact such as shock metamorphism. However, detailed analysis of the Neoproterozoic Mahe granite failed to detect any shocked quartz (A. Glikson, pers. comm.). Moreover, radiometric ages from the

drill core samples of basalt from the floor of the Amirante Basin basalt provided an Upper Cretaceous age (~80 Ma; Fisher et al. 1968), which was overlain by thick limestone bed containing Early Maastrichtian foraminifera (Johnson et al. 1982). Thus, the Amirante basin was formed somewhat earlier than the KT boundary event and cannot be part of the Shiva crater. Moreover, the Amirante Arc appears to be an inactive island arc, not a crater rim (Mart 1988). The cumulative evidence suggests that Amirante Basin can no longer be considered the southern half of the Shiva crater as proposed earlier (Alt et al. 1988; Chatterjee and Rudra 1996; Hartnady 1986). Instead, the Shiva crater appears to be preserved entirely within the Mumbai Offshore Basin (Chatterjee and Guven 2002). At the time of the Shiva impact at the KT boundary time, India was connected to the Seychelles and Greater Somalia to form the Indo-Seychelles-Greater Somalia plate (Chatterjee and Scotese 1999) (Fig. 2). In this paper we redefine the boundary and extent of the Shiva crater on the basis of new evidence.

The western continental margin of India is an Atlantic-type passive margin, differentiated into four structural and sedimentary basins from north to south: the Kutch, Mumbai, Konkan, and Kerala Offshore basins containing large oil and gas fields (Biswas 1987). The Shiva crater, located on the Mumbai Offshore Basin, was discovered in 1974 using seismic data and is bounded by several fault and rift systems. The stratigraphy, structure, tectonic framework, geophysical characteristics, facies distribution, petroleum geology, and depositional history of the Shiva structure are known primarily from the exploration work in the Mumbai Offshore Basin by the Oil and Natural Gas Commission (ONGC) of India and described in several reports (Basu et al. 1982; Bhandari and Jain 1984; Biswas 1987; Mathur and Nair 1993; Mehrotra et al. 2001; Rao and Talukdar 1980; Zutshi et al. 1993). Our interpretation of the Shiva crater is largely based on the published literature by the workers of the ONGC.
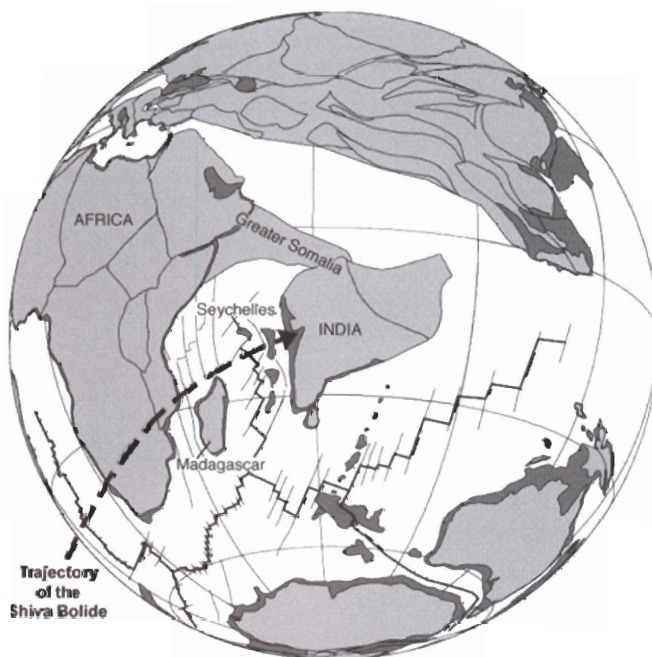

Figure 2. Paleogeographic position of India-Seychelles-Greater Somalia block during the KT boundary (~65 Ma) when a large bolide, about 40 km diameter, crashed on the western shelf of India to create the Shiva crater (modified from Chatterjee and Scotese 1999).

MORPHOLOGY AND SIZE OF THE SHIVA CRATER

Impact structures are recognized by their crater morphology and by the physical and chemical effects of impact. Terrestrial impact craters appear to display a regular progression of crater morphology from small simple craters, through complex central peak and peak-ring craters, to large multi-ring crater basins (Grieve 1990; Melosh 1989). A simple crater is a bowl-shaped depression with a raised rim, as illustrated by the Barringer crater in Arizona; it is generally less than a few kilometers across. With increasing diameter (>4 km across), a complex-type crater develops, with a distinct central peak, annular trough, and a collapsed outer rim. As crater size increases, a peak ring, typically an irregular ring of hills and massifs that lacks prominent asymmetric bounding scarps, replaces this central peak. With further increase in crater size, peak ring craters evolve into multiringed basins, as commonly seen on the surfaces of the Moon and Venus.

The Shiva structure has an irregular shape, more squarish than circular like the Barringer crater, with a diagonal of 500 km, and is defined by large peripheral boundary faults. Melosh (1989) explained how joints, faults, and planes of weaknesses in the target rock, as well as the angle of impact, could modify the crater shape from typical circular to various shapes, such as rectangular, elliptical, polygonal, multiring, and aberrant basins. The unusual squarish shape of the Shiva structure possibly reflects an intersecting set of boundary faults (Fig. 3).

We interpret the morphology of the Shiva crater as a complex multiringed basin, defined by the collapsed outer rim in the form of faulted margin with an elevated rim around the perimeter. The eastern border of the crater lies on the Indian continent and is bordered by the Panvel Flexure, whereas the northern border is limited by the Narmada Fault in the Arabian Sea (Chatterjee and Rudra 1996); the Kori Arch bounds the western border, and the Ratnagiri fault delineates its southern border (Fig. 3). The crater rim is followed inward by the annular trough, which was largely filled with thick Cenozoic sediments. The annular trough is preserved in the shape of the Surat Depression, Saurasthra Depression, Shelf Margin Depression, Murad Depression, and the Panna Depression. An inner concentric ring comprised of irregular mountain peaks on the Bombay High-Deep Continental Shelf (DCS) block replaces the central peak. It is separated from the annular trough by a circular thrust fault. The inner peak ring diameter is about 200 km, roughly half the rim-to-rim diameter of the crater. Such peak-ring craters have been recognized on the Earth, Moon, Mars, and Mercury, with similar morphology and similar diameter of the inner and outer ring ratios (Melosh 1989). The peak ring consists of several subsurface mountains including the Bombay High, Mukta High, Panna-Bassein High, Heera High, and several other unnamed peaks, which stand several kilometers above the surrounding basement. Based on seismic data and well data each peak consists of a core of Neoproterozoic granite, which was overlain by a veneer of Deccan trap and thick Cenozoic sediments (Fig. 3).

In addition to its peak ring, at least three different ring structures have been identified. A circular faulted rim with a diameter of 250 km borders the peak ring that probably marks the position of the transient cavity rim. From this second rim, the beginning of the annular trough can be seen outwardly, and is filled with 7-km-thick Cenozoic sediments. A third ring, about 500-km-diameter, represents the final faulted rim of the crater. This is bordered by a raised margin represented by the Saurashtra Arch, Kori Arch, and the Ratnagiri Arch in the Arabian Basin, which may represent the fourth ring. If the outermost fourth ring with a topographic high locates the final crater rim, the Shiva has a crater diameter of 550 km instead of 500 km (Fig. 3).

It is generally accepted that multi-ring basins result from very large impacts, but the mechanism by which they form is being debated (Melosh 1989). Most of what is currently known about multi-ring basins is based on remote-sensing studies of the Moon, Mars, and Mercury. If our interpretation is correct, Shiva is the most pristine and largest impact crater known on Earth and one of four known multi-ring terrestrial craters with the Vredefort, South Africa, Sudbury, Canada, and Chicxulub, Mexico craters being the other three.

Mathur and Nair (1993) provided a series of stratigraphic cross-sections of the Mumbai Offshore Basin across the Bombay High field. Two of these cross-
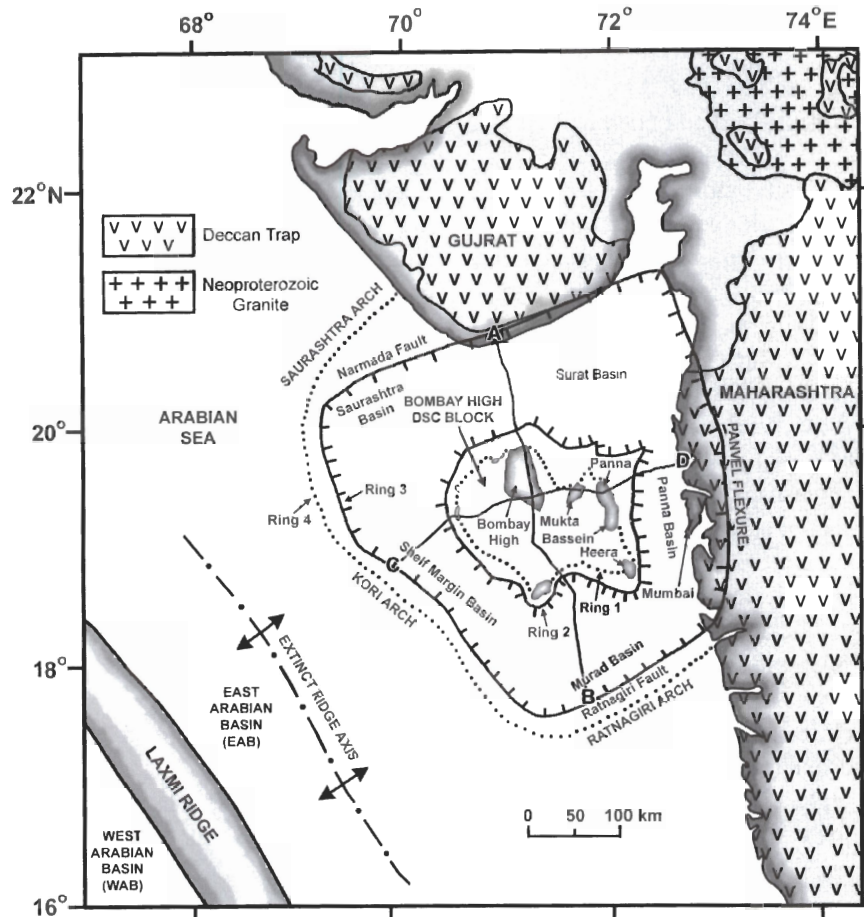
Figure 3. Present day location of the Shiva crater at the Mumbai Offshore Basin, western shelf of India. The Shiva structure is a complex peak ring crater and a multiring basin, about 500 km across, which is buried by 7-km thick Cenozoic sediments. The crater is defined by a peak ring, annular trough, and the faulted outer rim. A small segment of the eastern part of the crater lies near the Mumbai coast, which is bordered by the Panvel Flexure; here the crater floor is overlain by 2-km thick Deccan lava pile. Four different ring structures have been identified. The inner peak ring (Ring 1) is about 200 km diameter, and consists of several structural highs including Bombay High, Mukta High, Panna-Bassein High, Heera High, and several unnamed peaks. The peak ring is the structural trap for oil and gas. The peak ring is followed by a circular faulted rim (Ring 2), with a diameter of 250 km, and is bordered by the annual depression consisting of several basins such as Panna Basin, Surat Basin, Saurashtra Basin, Shelf Margin Basin, and Murad Basin, where the crater fill Cenozoic sediments exceed 7 km in thickness. The annular basin is bordered by the faulted crater rim (Ring 3), about 500 km, consisting of Panvel Flexure, Narmada Fault, Shelf Margin Fault, and the Ratnagiri Fault. Finally, the faulted rim is probably bordered by the raised rim of the crater (Ring 4), about 550 km in diameter, represented by the Saurasthra Arch, Kori Arch, and the Ratnagiri Arch in the Arabian Sea. A-B and C-D show the regional cross-section lines across the crater, which are shown in Figure 4. The enigmatic Laxmi Ridge, a continental sliver about 700 km long and 100 km across in the Arabian Sea, lies west of the Shiva crater (modified from Chatterjee and Rudra 1996; Mathur and Nair 1993; Talwani and Reif 1998; Zutshi et al. 1993).

sections, N-S and E-W across the Bombay High, are shown in Figure 4, where the overlying Tertiary sediments were removed to expose the topography of the floor of the Shiva crater. The structural relief of the crater, from the lowest to the highest point of the central peak. exceeds 7 km at Saurashtra Basin in the northwestern corner of the crater (Mathur and Nair 1993).

Seismic stratigraphy and well drilling have identified the basement rock as the volcanic lava flows of the Deccan Traps that forms the undulating basin, with few inliers of Neoproterozoic granite that form the ring peaks of the Shiva crater. Apparently, the target rocks were both Neoproterozoic granite and the overlying Deccan Trap. The thickness of the Neoproterozoic basement rock, the Deccan lava floor, and the Deccan Trap breccia unit within the crater are unknown from published accounts. Thus, the total

vertical rebound of the central peak cannot be estimated at the moment. The uplift in the center of a complex crater amounts to about one tenth of the crater's final diameter (Grieve 1990). Thus, the uplift associated with the 500-km-wide Shiva crater is estimated to be 50 km. Geophysical anomalies indicate that the lithospheric mantle in this region has been considerably fragmented, sheared, and deformed around Shiva crater, whereas the crust-mantle boundary has been uplifted more than 50 km. These unusual geophysical anomalies, discussed later, have been attributed to an impact event and indicate the amplitude of the uplift (Pandey and Agarwal 2001). The crystalline rocks beneath the Shiva crater are shattered and broken to a great depth, inferred from seismic velocity beneath the crater and low gravity anomalies (Rao and Talukdar 1980; Srivastava 1996).
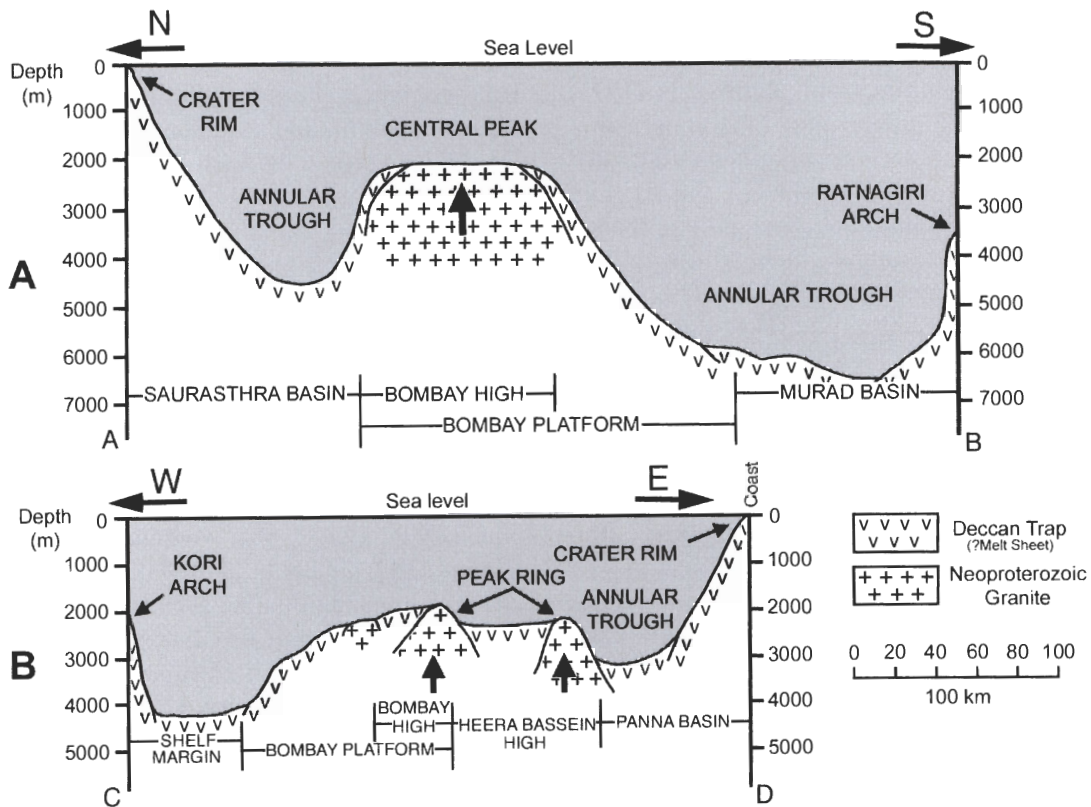

Figure 4. Cross-sections across the Shiva crater to show the relief of the crater basin; the overlying Cenozoic sediments were removed (see Figure 3 for reference). A, north-south cross section (A-B line) from Saurashtra coast to Ratnagiri Arch; B, west-east cross section (C-D line) from the Kori Arch to Mumbai coast (modified from Mathur and Nair 1993).

STRATIGRAPHY AND AGE

The subsurface stratigraphy of the Shiva crater is known primarily from petroleum exploration of drill holes and geophysical anomalies data (Basu et al. 1982; Bhandari and Jain 1984; Mathur and Nair 1993; Rao and Talukdar 1980; Wandrey 2004; Zutshi et al. 1993). The sedimentary fill in the depocenter consists of nearly horizontal strata of Cenozoic sediments, Paleocene to Holocene in age, representing a typical shallow marine shelf sequence exceeding 7 km in thickness. The basin accumulated large volumes of shallow marine carbonates, shales, siltstones, and sandstones. Thick piles of Early Eocene to Middle Miocene carbonate sediments dominate the lithology of the basin. These depositional environments fluctuated but prevailed until the Holocene. Presence of larger benthic foraminifera in most of the Cenozoic sections and lack of planktic forms suggest a warm, shallow-water marine or lagoonal environment in the crater basin. The Cenozoic formations of the crater basin include in ascending order, the Panna, Bassein, Alibag, Ratnagiri, and Chinchini. Zutshi et al. (1993) provided the seismic stratigraphy of this crater basin. It shows five seismic reflection marker beds, designated from bottom to top as H5, H4, H3, H2, and H1 (Fig. 5). The H5 seismic horizon is reflection-free, chaotic zone, probably representing the highly fractured floor of the crater basin consisting of Deccan Trap basalts and Neoproterozoic granite. The H4 seismic horizon coincides with the top of the Panna Formation.

The Panna Formation, the lowest unit of Tertiary sediments, lies unconformably on a thick layer of breccia embedded in reddish claystone and siltstone, referred to here as the 'Deccan Trap Breccia.' The breccia unit, in turn, overlies either the Deccan lava pile or the Neoproterozoic granitic basement of unknown thickness. Since the age estimates for the Deccan lavas in western India cluster around 65 Ma (Courtillot 1990; Duncan and Pyle 1988), it is suggested here that the Deccan Trap Breccia unit, sand-

wiched between the Early Paleocene Panna Formation and the Deccan Trap, indicates impact-related sedimentary deposits at the KT boundary.

The Panna Formation, overlying the KT boundary sequence, is composed of poorly sorted, angular sandstone and claystone at the bottom followed by shale, limestone, and coal sequences. This unit is relatively thin on the central uplift, but becomes relatively thick on the flank (~75 m). Seismic data indicate this formation to be as thick as 500 m in the deeper part of the basin in the annular trough, such as the Saurashtra basin. Although the Panna Formation is mostly unfossiliferous, it has yielded *Globorotalia pseudomenardii* from the middle of the sequence corresponding to the P4 planktic foraminiferal Zone of the Late Paleocene (Basu et al. 1982). The occurrence of nummulite fossils such as *Nummulites deserti* and *Assilinia spinosa* also support similar Thanetian age of the Late Paleocene (Rao and Talukdar 1980). However, recent biostratigraphic analysis suggests that the lower part of the Panna Formation may extend to the Danian Stage of the Early Paleocene (Zutshi et al. 1993).

The available stratigraphic information is consistent with the formation of the Shiva structure at about 65 Ma. The lack of Cretaceous or older sediments clearly indicates that the crater basin was formed at post-Cretaceous time. The Deccan Trap breccias may be linked to the impact event, followed by the deposition of Early Paleocene Panna Formation. The two units bracket the age of the crater basin at the KT boundary interval. Earlier workers (Basu et al. 1982; Biswas 1987; Zutshi et al. 1993) reached a similar conclusion regarding the KT boundary age for the structure of the Mumbai Offshore Basin. A radiometric age (~65 Ma) of the crater formation is provided by the impact melt rocks as discussed later.

EVIDENCE OF IMPACT WITHIN A CRATER BASIN

In addition to the complex crater morphology, direct and indirect evidence within the crater basin is compatible with the hypothesis that the Shiva struc-

ture was created by a bolide impact. Most ejecta from the impact cratering processes are emplaced ballistically by the flight of the debris expelled from the cra-

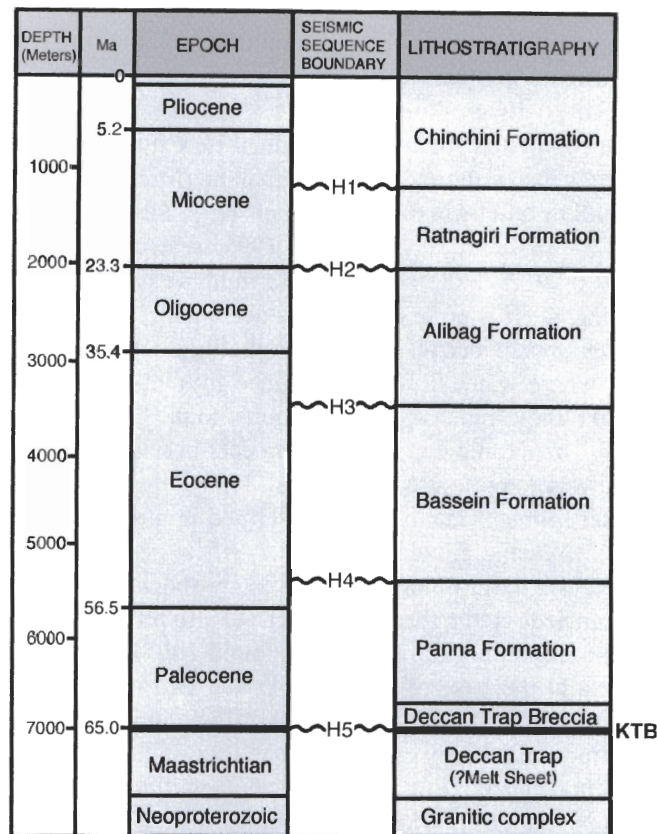| DEPTH (Meters)	Ma	EPOCH	SEISMIC SEQUENCE BOUNDARY	LITHOSTRATIGRAPHY
0		Pliocene		
	5.2			Chinchini Formation
1000		Miocene	~H1~	
				Ratnagiri Formation
2000	23.3		~H2~	
		Oligocene		Alibag Formation
3000	35.4			
			~H3~	
4000		Eocene		Bassein Formation
5000				
			~H4~	
	56.5			Panna Formation
6000		Paleocene		
				Deccan Trap Breccia
7000	65.0		~H5~	Deccan Trap (?Melt Sheet)
		Maastrichtian		
		Neoproterozoic		Granitic complex

Figure 5. Generalized stratigraphy of the Shiva crater (modified from Basu et al. 1982; Bhandari and Jain 1984; Mathur and Nair 1993; Rao and Talukdar 1980; Wandrey 2004; Zutshi et al. 1993). The oldest sedimentary units in the crater basin, the Deccan Trap breccia, the early Paleocene Panna Formation, and the Deccan Trap floor, bracket the age of the crater at the KT boundary time.

ter interior. However, some ejecta from the crater wall and rim slump back to the annular trough and form important crater filling units. The Shiva impact must have produced enormous volumes of crater-filling units, such as impact breccias and impact melts. Because much of the drill cores from the crater basin are proprietary, the nature and extent of the crater-filling ejecta and melt cannot be determined at this stage. The basement rock of the basin is often interpreted as the Deccan Trap. Could it be actually impact melt rock? Without further petrographic analysis two alternatives cannot be tested. We believe that the impact was so intense that lava-like fluid ejecta bodies were emplaced radially within and outside the crater,

but their relationships, compositions, distribution, and relative stratigraphic positions suggest possible relationships to stages of crater excavation and collapse. Impact lithologies such as breccias and impact melt rocks are physical and chemical mixtures of pre-existing target lithologies. From the lithology of the floor of the Shiva crater it appears that the target rock was composite: the Neoproterozoic crystalline basement overlain by the older flow of the Deccan Trap.

Deccan Trap Breccia. —Impact on a continental target rock generally preserves a thick sequence of crater-filling ejecta units such as in the Ries crater of Germany (Hörz 1982) and the Manson crater in Iowa

(Koeberl and Anderson 1996). Breccias associated with the Ries crater of Miocene age are probably the best-studied impact deposits presently known. Two general types of impact-related deposits are known from Ries: (1) the Bunte Breccia comprised predominantly of clasts of sedimentary target materials; and (2) suevite, containing clasts of crystalline basement rocks and impact-melt rock.

A large impact on an oceanic shelf is quite different from a continental target impact because it would generate a megatsunami where water flow in and out of the crater cavity would remove much of the ejecta components from the basin. In oceanic impacts some of the fall-out breccia is reworked back into the crater basin. This is why the crater-filling ejecta in the Chicxulub and the Shiva are not significant. Emplacement of this breccia within the crater basin involved dynamic processes related to transient crater formation and collapse and to early post-impact filling (Grieve 1990). The Deccan Trap breccia at the base of the Panna Formation is a sedimentary-clast breccia, dominated by fragments of Deccan Traps and their weathered products in the form of clay matrix (Fig. 5). However, the thickness and composition of this breccia are not known (Basu et al. 1982). Unfortunately, this breccia unit has never been investigated for cosmic signatures such as iridium anomalies, shocked quartz, spherules, and impact melt rocks.

Deccan Traps/Impact Melts at the Floor of the Shiva Basin.—During large impact cratering processes, postshock temperatures are sufficiently high to cause whole rock melting of the target, leading to the formation of impact melts within the crater basin (Grieve 1998). The peak ring of the Shiva crater is underpinned by elevated volcanic rocks referred to as "Deccan Traps" (Basu et al. 1982) that lie between the breccia unit and the Neoproterozoic granite (Fig. 5). Boreholes drilled by ONGC within the Shiva crater have penetrated thick (~7 km) Tertiary sediments, and at places the underlying basalts are known, based on seismic data, to be over 4 km thick (Mahadevan 1994). In contrast, the greatest thickness of the Deccan Trap in Indian subcontinent is about 3 km in the Western Ghats section. We speculate that such a thick lava pile (~ 4 km) in the crater basin may indicate impact-generated melt sheet rather than lavas of the Deccan volcanics. Petrographic analysis of the cored samples

may settle the genesis of this enigmatic lava sheet in the future.

Pseudotachylite.—Pseudotachylite is a dark, fine-grained rock that resembles volcanic glass. It forms in characteristically high strain rates such as seismic events (e.g., Sibson 1975) or bolide impacts (Fiske et al. 1995) where many variables including lithology, pore-fluid pressure, ambient temperature, and strain rate act to generate a melt phase during the event. The morphology of impact-generated pseudotachylite is defined by mm-scale vein networks of dark glass in contrast to the larger (cm-scale), anastamosing lenses that occur in seismically related fault zones (e.g., Fiske et al. 1995). Impact-related pseudotachylites were first described in association with the Vredefort crater in South Africa, where they were interpreted to be produced by shock compression and release during impact and also providing the timing for the impact event (Reimold 1995). Cores of Neoproterozoic granitoid rocks (target rock) derived from petroleum exploration drilling under the Bombay High area contain evidence for cataclasis (rock pulverization) and probable pseudotachylite veins. Petrographic studies of two samples display discordant veins 400-1000 microns thick of aphanitic, micro- to cryptocrystalline material that intrude into feldpsar crystals within a mylonitized feldspathic gneiss (Fig. 6A, 6B). Inclusions of feldspar aggregates are observed within the aphanitic groundmass. These textures and intrusive relationships are consistent with experiments that have produced shock-melted glass during impact (Fiske et al. 1995) and field/petrographic studies of pseudotachylite (e.g., McNulty 1995). SEM images and Energy-dispersive X-ray spectra (EDXS) indicate that the composition of the pseudotachylite is pure silica glass (Fig. 6C). It is likely that the silica melt rock is the result of shock pressure induced by the Shiva impact.

Rhyolite Dikes.—Melt rocks, which are created by strong shock waves that emanate from the site of the impact, are very common near large impact craters. We hypothesize that two distinct impact melt rocks coexist in and around Shiva crater–'white' and 'black' impact melts—because of involvement of two distinct target lithologies: Neoproterozoic granite and Deccan Trap. The former gave rise to 'white' rhyolite dikes that are more restricted in distribution due to high viscosity and confinement within the crater ba-
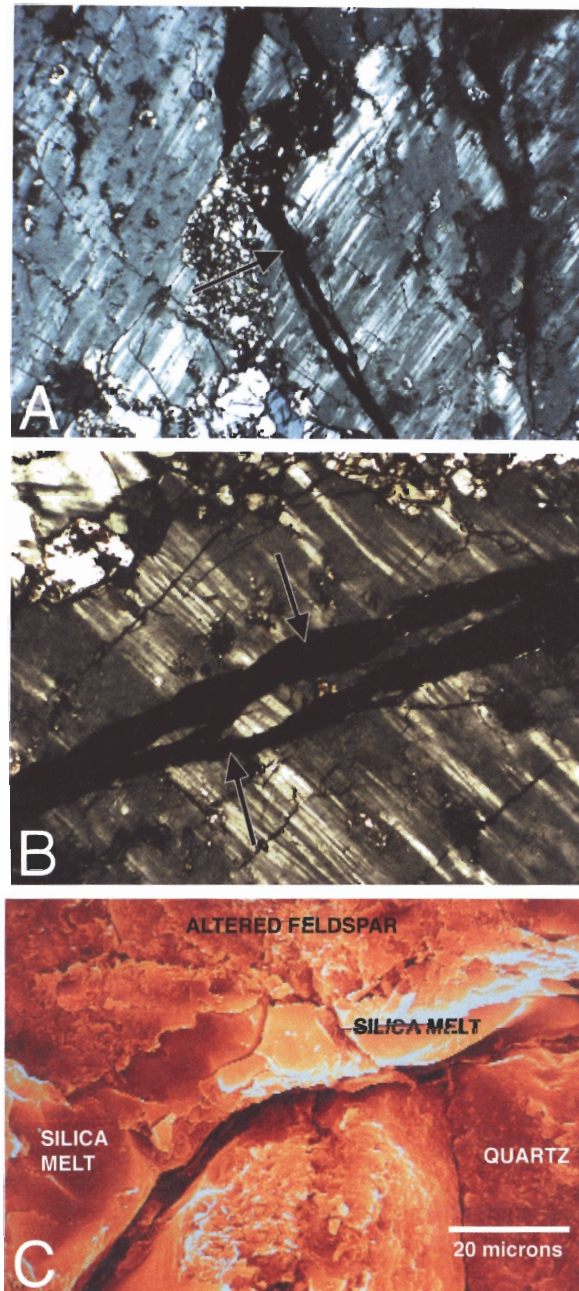
Figure 6. Pseudotachylite veins of the basement granite drill core from the Shiva crater. A-B, thin section micrographs of basement granite (crossed nicols), showing thin vein of pseudotachylite cutting across K-feldspar grain. The granite hosting the pseudotachylite is strongly shock metamorphosed by the impact. C, SEM photograph of the basement granite showing the highly magnified view of the pseudotachylite vein containing pure silica melt. The impact was so powerful (> 100 GPa) that it obliterated the PDFs of shocked quartz grain and turned it into a melt component.

sin; the latter is more extensive because of low viscosity with meteoritic contamination and represents the 'black' alkaline igneous complexes that were emplaced outside the crater rim as fluid ejecta noted in lunar craters; both kinds of melt rocks were emplaced within the Deccan Trap (Fig. 7). Similar bimodal impact melt rocks are known from the Wabar crater, Saudi Arabia (Hörz et al. 1989).

The Deccan lava pile obscures the floor of the Shiva crater from observation on the continent near the Mumbai coast, west of the Panvel Flexure. It is thickest along the Western Ghats region (~2000 m) but thins progressively inward in an eastern direction. Considerable volumes of acid and basic tuffs, and rhyolite and trachyte lava dikes associated with the Deccan lava pile, occur within the crater basin along the Mumbai coast. But their origin is still debated, ranging from partial melting of the granitic basement rock (Sethna 1989) to partial melting of basic rocks (Lightfoot et al. 1987). Direct derivation of these rhyolite and trachyte dikes from the mantle would appear to be precluded by their silica-rich nature. The ages of these felsic dikes straddle the ~65 Ma KT boundary (Sheth and Ray 2002) and may have erupted in response to impact melting of the basement target rock. The Neoproterozoic granite appears to be the target rock as indicated by geophysical anomaly indicating the presence of unusually thin crust in the Mumbai area with missing granitic layer. The pseudotachylite veins observed within the drill core samples of the Neoproterozoic granite may be genetic and temporal extension of the rhyolite dikes.

Geophysical Anomaly.—The western coast of India, though a passive plate margin, is seismically very active, indicating large-scale geodynamic instability (Ramalingeswara Rao 2000). This part of the Indian plate has been associated with several major geodynamic and tectonic events at the KT boundary time, including Deccan volcanism, impact, continental breakup, and seafloor spreading. Although extensive geophysical investigations have been carried out by the ONGC around the Bombay High because of oil
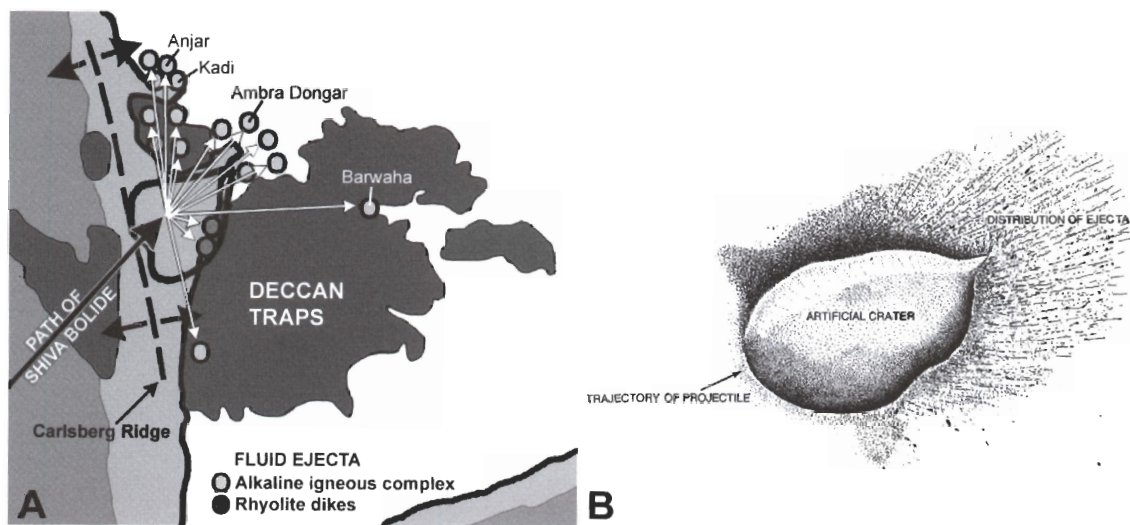

Figure 7. A, radial, asymmetric distribution of fluid ejecta downrange of the Shiva crater; teardrop shape of the crater and asymmetric distribution of melt rocks consistent with the oblique impact model along the NE downrange direction; alkaline igneous complex rocks were emplaced outside the crater rim, whereas rhyolite rink dikes are restricted within the crater rim; arrow indicates the trajectory of the meteorite; similar asymmetric distribution of fluid ejecta are known from craters of Moon, Mars, and Venus. B, artificial crater produced by low-angle (~15°) oblique impact in the laboratory mimics the shape and fluid ejecta distribution of the Shiva crater (simplified from Schultz and Gault 1990).

exploration, very few data have been published. One of the rare published accounts is the satellite-derived gravity data over the Bombay High area, which can be found in the annual report of ONGC (Srivastava 1996). The geophysical expression of the Bombay High area is similar to the central peak ring in other large impact craters (Fig. 8). The most notable geophysical signature associated with terrestrial impact structures is a negative gravity anomaly (Grieve 1998; Pilkington and Grieve 1992). Fracturing and brecciation of hundreds of meters of basement rocks inside the impact basin caused by the impact, produce a characteristic negative gravity anomaly at the central peak reflecting a mass of low-density material. These gravity lows are generally circular and typically extend to, or slightly beyond, the outer rim of the structure.

Gravity data of the Shiva crater show a major gravity low anomaly over the central peaks of the Bombay High region similar to the pattern of the Chicxulub crater (Hildebrand et al. 1995). The peak ring has a clear gravitational signal. The Bouguer anomaly values reach extreme lows of -15 mgal at the center of the crater and -5 mgal over the central peak-ring, which gradually rise toward the crater rim about +40 mgal, and become highs as much as +50 mgal at the Mumbai coast, but show lower values in the western rim of the crater. The cause of the high gravity anomaly near the Mumbai coast is discussed in a later section. The negative anomalies around the peak-ring correspond to the relatively low densities of the uplifted core of the lighter Neoproterozoic granite, overlain by the Tertiary sediments filling the crater. They may also reflect mass deficiency such as fractured crystalline basement rock beneath the crater. We speculate that the central peak-ring of the Shiva crater consisting primarily of Neoproterozoic granite surrounded by the denser Deccan Trap basalt, may explain the gravity gradient within the crater.

The most striking gravity feature near the Mumbai coast is the high Bouguer anomaly that may be linked to a large intrusive of alkaline igneous complex of impact melt, called the 'Napsi' structure (Chatterjee and Rudra 1996), which is about 12 km high, has a maximum diameter of 35 km at the base, and is linked to the impact (Negi et al. 1993; Pandey and Agarwal 2001). In this region, the Panvel Flexure, an arcuate feature that bounds the eastern rim of the crater, is about 120 km long and formed around 65 Ma (Sheth 1998). It is
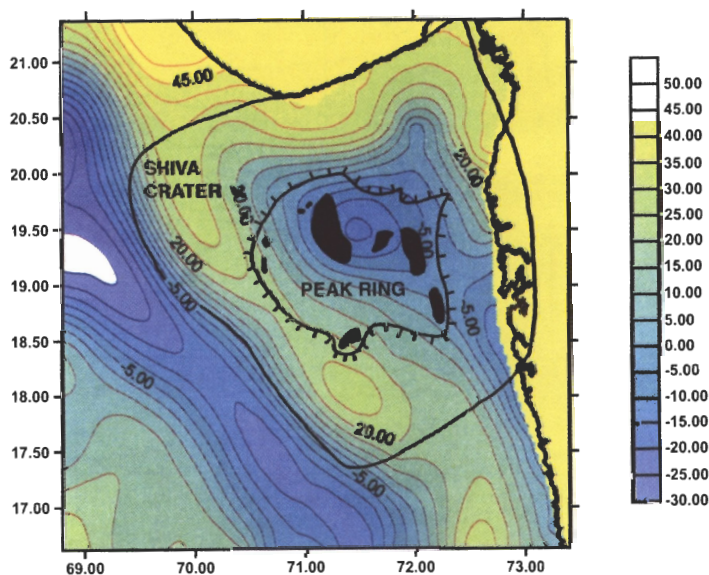

Figure 8. Satellite-derived gravity over Shiva crater from closely spaced repeat passes of ERS-altimeter shows a distinctive low gravity anomaly (-5 mgal) over the central peak ring; it gradually rises toward the crater rim (+40 mgal) as in other impact craters (modified from Srivastava 1996).

marked by a line of hot springs, dikes, deep crustal faults, and seismicity, where the floor of the crater slopes westerly toward the offshore basin (Kaila et al. 1981). It exercises a tectonic control on the attitude of the Deccan lava pile. To the east of the flexure, the basaltic flows are horizontal; to the west of the flexure, the basaltic flows dip west to west-southwest at 50°-60° toward the coast. The abrupt change of dip along the flexure axis may indicate the slope of the crater wall, which is concealed by the thick Deccan lava flows (Fig. 9) (Chatterjee 1992).

Geothermal Anomaly.—Pandey and Agarwal (2001) studied in detail the gravity, geothermal gradient, and heat flow distribution beneath the western continental margin of India around the Mumbai coast. They estimated the average heat flow at the eastern margin of the crater, which lies on the continental crust but is covered by a thick pile of Deccan lava, to be very high (>80 mW/m²). They conclude that the lithospheric mantle beneath this part of the Shiva crater has been considerably sheared, thinned, deformed, and weakened due to mantle upwelling with a missing granitic layer (Fig. 9). They attributed this anomalous high heat flow and mantle upwelling to a possible catastrophic and geodynamic event around 65 Ma, such as the Shiva impact. The uplift of the geotherms accompanying the collapse of the giant Shiva crater might lead to pressure release melting of deep mantle/asthenosphere layers and create the large Deccan igneous provinces. Elkins-Tanton and Hager (2005) proposed a model for impact-triggered Deccan volcanism in which the cratered lithosphere could rise isostatically into a dome (Fig. 9), as seen in the west coast of India, warp-
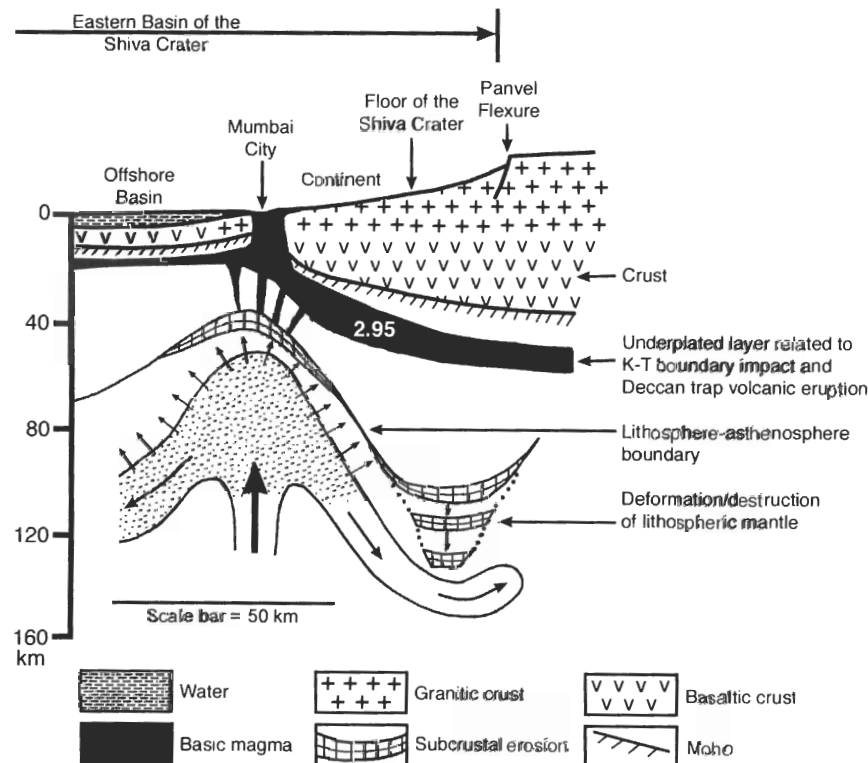

Figure 9. Schematic diagram of the eastern part of the Shiva crater near Mumbai coast to show the upwarping of the mantle more than 50 km and the possible deformation and destruction of the lithosphere because of Shiva impact; on the right side of the drawing, east of Mumbai, thick Deccan lava pile was removed to show the floor of the Shiva crater (modified from Kaila et al. 1981; Pandey and Agarwal 2001).

ing isotherms at the lithosphere/asthenosphere boundary, in which adiabatic melting could occur.

The mantle upwelling dome at the Mumbai coast does not coincide axially with the crater peak ring, but is displaced more easterly toward the coast. We attribute this offset of the thermal anomaly as due to an oblique impact event (discussed later) where the eastern rim of the crater was more severely affected because of the downrange direction of the bolide trajec-

tory; this view also is supported by the asymmetric distribution of the fluid ejecta (Chatterjee and Rudra 1996). Existence of two such gravity anomalies of opposite nature, one above the peak ring, the other nearly above the crest of the mantle upwelling separated by a distance of only 160 km, is intriguing and suggests complex geodynamic activity due to an oblique impact and its unequal stress distribution in the lithosphere in the region.

AGE OF THE DECCAN TRAPS

Very rapid emplacement of the Deccan traps has been one of the key arguments for its catastrophic role in the KT mass extinction. The outpouring of the enormous continental flood basalts of the Deccan Trap,

spreading over vast areas of western and central India and the adjoining Seychelles microcontinent covering more than 1,500,000 km^2, also marked the close of the Cretaceous time (Figs. 7, 10). The lava pile is the

Figure 10. Paleoposition of India-Seychelles during the KT boundary time showing the location of KT boundary sites around the Deccan volcanic province (grey circles). The KTB sites containing cosmic ejecta in India, from west to east are: Anjar, Gujrat; Barmer, Rajasthan; Jabalpur, Madhya Pradesh; Um Sohryngkew, Meghalaya; and Ariyalur, Tamil Nadu (modified from White and McKenzie [1989] and other sources).

thickest in the western part of the Deccan volcanic province, reaching an exposed thickness of about 2 km in parts of Western Ghats, but becomes gradually thin in the east, where it attains no more than about 100 m. Chatterjee and Rudra (1996) reviewed the age of the Deccan traps on the basis of geochronologic, paleomagnetic, and paleontologic constraints. ^{40}Ar/^{39}Ar dates of the stratigraphically controlled thick sequences of Deccan lava piles around the Western Ghats section cluster around a narrow span of age from 64.4 to 65.3 Ma, with a major eruptive phase around 65 Ma, coinciding with the KT mass extinction (Courtillot 1990; Courtillot et al. 1988; Duncan and Pyle 1988; Hofmann et al. 2000; White and McKenzie 1989). Thus this enormous volcanic mass had been laid down

in less than 1 Kyr. Paleomagnetic studies in the thick Western Ghats section indicate that Deccan volcanism began during the 30N magnetic chron, climaxed during the following reversed interval 29R at the KT boundary, and ended in the 29N chron (Courtillot 1990). In marine section, the lowest level of Deccan lava rests on a sedimentary layer that contains the typical Late Maastrichtian index foraminiferal fossil *Abatomphalus mayaroensis*, which thrived close to the KT boundary and then disappeared. It thus appears from the combined evidence of radiometric dating, paleomagnetic evidence, and fossil studies, that the estimated duration of Deccan volcanism is about 900 Kyr around the KT boundary (Fig. 11).
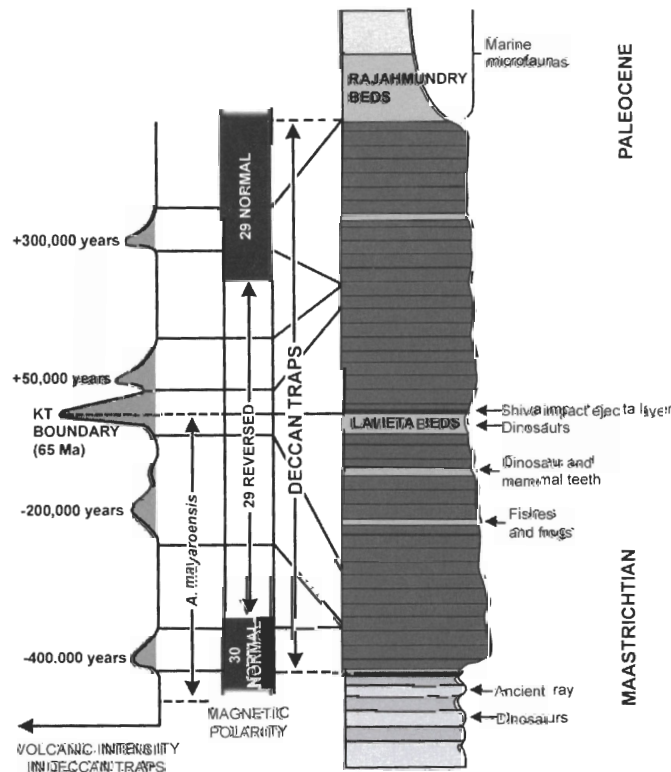

Figure 11. A synthesis of paleomagnetic, paleontologic, and geochronologic data from the Deccan Trap lava pile showing the stratigraphic position of the KT boundary and its relationships with the intertrappean beds such as Lameta Formation. Various cosmic signatures, such as iridium anomaly, high-pressure fullerenes, shocked quartz, Ni-rich spinel, magnetic nanoparticles, ejecta droplets, and fluid ejecta have been found from different KT boundary sec-tions of India, which are linked to the Shiva impact (modified from Courtillot 1990; Chatterjee and Rudra 1996).

The Deccan lava flows were not extruded all at once; volcanic activity was punctuated periodically when sedimentary beds were deposited between the flows. These fluvial and lacustrine deposits are called intertrappean beds that contain abundant remains of plants, invertebrates, fish, frogs, crocodilians, turtles, dinosaurs and their eggs, and mammalian teeth (Chatterjee and Rudra 1996). Many of these KT boundary sections are located within the intertrappean sedimentary layers, which are sandwiched between two Deccan flows. Thus, KT boundaries in India are well constrained stratigraphically and can be recognized by paleontologic evidence, radiometric age of the lava flows, and cosmic signatures. Impact debris contains variable concentrations of projectile and target materials that can be shocked, melted, or vaporized. Presumably, evolution of impact ejecta can occur over extended periods of time as these materials are transported, deposited, and interact with each other and atmosphere.

DISTRIBUTIONS OF SHIVA EJECTA AT THE KT BOUNDARY SECTIONS

There are several KT boundary (KTB) sections in India, particularly in and around Deccan volcanic province, which have yielded several cosmic marker horizons attributed to Shiva impact. The oblique impact of Shiva in a SW-NE trajectory caused multistaged ejecta emplacement downrange. Seven types of material have been interpreted as distal ejecta from the Shiva Crater. They include fluid ejecta, shocked quartz, iridium anomalies, highly magnetic nanoparticles, fullerenes, glass spherules, and Ni-rich spinels, which are believed to have come from different sources of the impact site. Iridium, Ni-rich spinel, magnetic nanoparticles, and high-pressure fullerenes probably came from vaporized meteorites, shocked quartz from unmelted basement granite, whereas ejecta layers and fluid ejecta came from the melted components of target rock. In addition, impact-generated tsunami deposits have been recognized in the Ariyalur section of Tamil Nadu. The widely separated KT boundary sections are difficult to recognize in the field because distal ejecta marker beds are usually represented by very thin stratigraphic horizons. Notable KT boundary sites in India containing evidence of impact ejecta horizons from west to east are: (1) Anjar section, Gujrat; (2) Barmar section, Rajasthan; (3) Jabalpur section, Madhya Pradesh; (4) Um Sohryngkew section, Meghalaya; and (5) Ariyalur section, Tamil Nadu (Fig. 10). Of these, the Anjar, Barmar, and Jabalpur sections are continental and are associated with the Deccan volcanic pile, whereas Um Sohryngkew is marine, and the Ariyalur section is mixed. These KT boundary sections with their ejecta components are described below along with the Deccan Traps.

Proximal Fluid Ejecta.—One of the most important effects of a large impact is the sudden conversion of nearly all of impactor's kinetic energy into heat to produce a vast volume of impact melts. Elkins-Tanton and Hager (2005) postulated three stages in the impact process that can create melt: (1) initial impact causes shock melt; (2) excavation of material from the impact site can cause instantaneous decompression melting beneath the impact site; and (3) development of a dome in the lithosphere-asthenosphere boundary either through instantaneous liquid flow of the shocked lithosphere or through later isostatic rebound. In and around Shiva crater, we can identify all three stages. We propose that the post-Deccan alkali igneous complexes represent the initial shock melt, which was emplaced radially as fluid ejecta. The bulk of the Deccan Traps, which erupted right at the boundary, might represent the second stage, the decompression melting process. The lithosphere/asthenosphere dome on the west coast (Fig. 9) adjacent to the Shiva crater probably represents the third stage of the impact-triggering process.

The impact-melt volumes generated from the 500-km diameter Shiva crater estimated from the crater scaling of Grieve and Cintala (1992) would be enormous, close to 10^6 km^3. These lava-like impact melts are very common at lunar craters and are emplaced downrange outside the crater rims (Howard and Wilshire 1975). Asymmetric distribution of fluid ejecta downrange indicates an oblique impact event. Lava like fluid ejecta outside the crater rims are rare on terrestrial craters, presumably because of their relatively

small size. However, the distribution of fluid ejecta of the Shiva impact outside the crater rims is analogous to the condition of large lunar craters.

One of the intriguing features associated with the Deccan flood basalt volcanism is the occurrence of several post-tholeiitic alkali igneous complexes of nepheline-carbonatite affinities along the radii of the Shiva Crater (Fig. 7). They are manifested in plug-like bodies and minor intrusions in the western and northwestern province and are limited in space and volume compared to the vast expanse of tholeiitic lavas (Bose 1980; De 1981). Basu et al. (1993) have recog-nized two pulses of eruption of these igneous complexes—early and late phases; one is pre-Deccan, the other is post-Deccan volcanism. They have shown that the Mundwara-Sarnu alkali igneous complexes, which are far outside these post-Deccan intrusives, were erupted at 68.5 Ma, which is about 3.5 Ma before the main phase of the Deccan eruption. These pre-Deccan alkali complexes have high $^3He/^4He$ ratio indicative of a plume origin. However, most of the spectacular plugs of alkali igneous complexes such as Anjar, Kadi, Jwahar, Phenai Mata, Amba Dongar, Barwaha, Murud, and Napsi structure are post-Deccan (Fig. 7A) with clearly defined zones of gravity highs (Biswas 1988). They probably represent impact melt fluid ejecta. The asymmetric distribution of fluid ejecta of these alkaline igneous complexes indicates a trajectory of the Shiva bolide from the SW to NE. Recent $^{40}Ar/^{39}Ar$ dating of some of these alkaline igneous complexes indicates 65 Ma, precisely coinciding with the KT boundary (Basu et al. 1993; Pande et al. 1988). Chatterjee and Rudra (1996) speculate that these volcanic plugs represent the fluid ejecta of the Shiva impact in the down range direction. Schultz and D'Hondt (1996) described similar asymmetric distribution of fluid ejecta resulting from an oblique impact that flowed down range at a distance more than the crater diameter (Fig. 7B).

There are several features that suggest the impact origin of the alkaline igneous complexes. First, Deccan lavas are poor in iridium content (~10 pg/g), but these post-Deccan alkali complexes are enriched with iridium (178 pg/g) (Shukla et al. 2001) and show evidence of crustal contamination (Basu et al. 1993; Paul et al. 1977). We speculate that the target rock for these alkaline igneous complexes were both early

phases of the Deccan Traps and crystalline basement granites, which were melted and contaminated by the asteroid impact as indicated by high iridium anomaly. Similar meteoritic contamination of impact melts is known from the Wabar crater, Saudi Arabia (Hörz et al. 1989). Second, impact melt rocks have higher K_2O/NaO ratios than the target rocks (Grieve 1987) as in the case of these alkaline igneous complexes. Third, the asymmetric radial distribution pattern of these alkaline complexes around the Shiva crater is expected in the downrange direction of fluid ejecta (Fig. 7). Fourth, they have restricted distribution and occur within Deccan volcanics as post-tholeiitic intrusives or plugs; they are conspicuously absent in other parts of the Deccan volcanic province. Fifth, their age matches exactly with the KT impact event.

Anjar KTB Section, Gujrat.—The Anjar volcano-sedimentary section in Gujrat is located at the western periphery of the Deccan flood basalt province and is probably the most thoroughly studied KT boundary section in India. It consists of nine lava flows (F1-F9) and at least four intertrappean beds (Bhandari et al. 1995). The third intertrappean bed, about 6 m thick (Fig. 12) occurring between F3 and F4, is well known for several cosmic signatures such as high concentrations of iridium (650-1333 pg/g) and osmium (650-2230 pg/g) (Bhandari et al. 1996; Courtillot et al. 2000), and fullerenes (Parthasarathy et al. 2002). Three thin limonitic layers are present in the lower 1.5 m of the third intertrappean bed, which is rich in iridium anomaly and fullerenes. These three iridium layers are designated as Br-1, Br-2, and Br-3, from top to bottom. Typical Late Maastrichtian fossil assemblages from this section include dinosaur bones and eggshells, microvertebrates, ostracodes, mollusks, and spores, which suddenly disappear just below the uppermost level of iridium layer (Br-1) indicating the mass extinction layer at the KT boundary. Fullerenes are also known from the Sudbury impact structure (Becker et al. 1994) and from the KT boundary sections of North America (Heymann et al. 1994) and are considered cosmic signature for impacts. The concentration of the high-pressure form of fullerenes (C_{60}) in other KT boundary sections of North America is low, about 0.41 ppm (Heymann et al. 1994), whereas in the Anjar section this value is three times high, about 1.3 ppm (Parthasarathy et al. 2002). Moreover, several lava flows of the Anjar section, F1, F2, F6, and F8, are
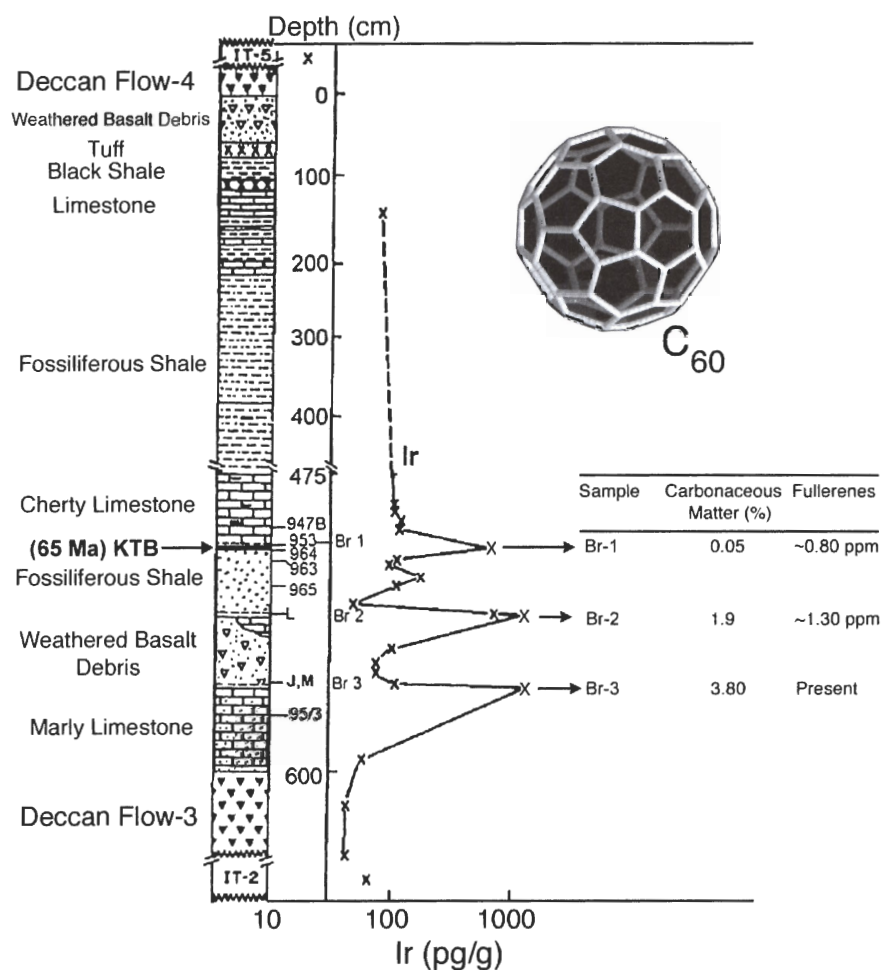
Figure 12. KT boundary section at Anjar, Gujrat, showing three closely spaced iridium and fullerene anomalies (Br-1, Br-2, and Br-3), which are sandwiched between two Deccan lava flows (F3 and F4) yielding 65 Ma radiometric age. From paleontologic evidence, Br-1 appears to coincide with the KT boundary. Three iridium and fullerene spikes may favor multiple impact hypothesis near KT boundary (modified from Parthasarathy et al. 2002).

rich in iridium concentrations as high as 178 pg/g (Shukla et al. 2001) and are interpreted as impact-generated fluid ejecta. The association of high-pressure, high-temperature forms of buckyball fullerenes, with high iridium concentrations, is a good indicator of an extraterrestrial impact, whereby the contaminated fluid ejecta in the Anjar section indicates proximate impact site. The occurrence of multiple levels of enriched iridium and fullerene in the Anjar section is puzzling. It may indicate either multiple impact events at the KT boundary as discussed earlier (Chatterjee 1997; Keller et al. 2003), where the Br-3 layer may correspond

with the Chicxulub impact event and Br-1 may coincide with the Shiva impact. Alternatively, three iridium layers may indicate reworking of the upper basaltic flow F4 due to secondary processes such as downward fluid mobilization in the Anjar area (Courtillot et al. 2000). However, Parthasarathy et al. (2002) discount this reworking hypothesis. Since iridium and fullerenes are insoluble in water it is unlikely that their coexistence in three different layers, separated by thick sediments, is due to fluid mobilization. These three iridium layers appear to be primary ejecta layers in-situ deposited in quick succession from different va-

porized meteoritic sources from different sites. If so, the Anjar section may hold the crucial evidence for three distinct episodes of global impact events during the KT transition. Similarly at the KT boundary section in Oman, two distinct iridium anomalies, separated by more than 1 m-thick sediments, mark the pre-KT and KT impacts (Ellwood et al. 2003). The Oman KTB section provides further proof of multiple impacts. There is growing evidence that multiple impacts occurred at the KT transition, including Chicxulub, Shiva, and Boltysh, which may correspond to the multiple iridium layers (Chatterjee 1997; Keller et al. 2003) (Fig. 1).

Recently, Bhandari et al. (2002) reported association of nanoparticles of magnetic and superparamagnetic iron oxide phases with iridium from the KT boundary section of the Anjar, which are attributed to impact origin. Apparently, these nanoparticles probably formed during condensation of the high-temperature impact vapor plume. Meteorites in general, have high concentrations of iron ($\geq 20\%$) in the form of silicates, metal, magnetite, and other iron-bearing minerals. Bhandari et al. (2002) reported similar cosmic magnetic particles from KT boundary sections of Meghalaya and other parts of the world.

Barmer KTB Section, Rajasthan.—A thin (~4 cm) unconsolidated layer of siliciclastic deposit at the KT boundary section of Barmer Basin, Rajasthan, in asso-ciation with early phase of the Deccan volcanism, contains several distal ejecta components such as Ni-rich vesicular glasses, sanidine spherules, shocked magnesioferrite spinels, and soot (Sisodia et al. 2005). The siliciclastic deposit disconformably overlies the Late Cretaceous shallow marine Fategarh Formation and is overlain by the Akli Formation of Paleocene-Eocene age (Fig. 12B). The igneous intrusive rocks within Fategarh Formation have yielded radiometric age ranging from 68 to 65 Ma, close to the KT boundary age (Basu et al. 1993). Sisodia et al. (2005) recognized glass shards, quartz beads, ferruginous hollow spheroids, and other melt ejecta components from this bed under microscopic examination. They point out that high nickel concentration (0.5 to 2% Ni) in glass spherules is generally considered as an indicator of an extraterrestrial component because of its high abundance in various types of meteorites and low concentration in terrestrial sources. They interpret this

siliciclastic deposit as possible ejecta or volcanic components having originated through a combination of ballistic and debris flow deposit. They argue that some ejecta particles such as sanidine spherules and skeletal magnesioferrites are petrographically very similar to those found around the Gulf of Mexico associated with the Chicxulub crater (Smit 1999). Magnesioferrite spinel crystals from the Barmer section occur as micrometer-sized skeletal forms. Their composition, small size, and skeletal morphology suggest they are condensation products of a vaporized bolide (Bohor 1990). Similarly, sanidine spherules from the Barmer section also indicate a large impact event (Smit and Klaver 1981). We believe that the boundary layer at the Barmer section is impact-related because it is rich in Ni-rich glass spherules, sanidine spherules, and skeletal magnesioferrite as seen in other KTB sections; we discount the volcanic origin proposed by Sisodia et al. (2005) because it lacks a coherent assemblage of volcanic crystals such as xenoliths and xenocrysts, which are common in ash-flow tuffs (Izett 1990). Thus the ejecta components from the Barmer section may imply remnants of hot, early ejecta from the nearby Shiva impact.

Jabalpur KTB Section, Madhya Pradesh.—The KT boundary section in Jabalpur represents the uppermost unconsolidated sandstone layer (~2.7 m) of the Lameta Formation and is overlain by the Deccan flow. The Lameta Formation has yielded various Late Maastrichtian dinosaurs such as abelisaurs and titanosaurs (Chatterjee and Rudra 1996). Chatterjee (1992) reported iridium levels of 0.1 ppb in the uppermost sandstone unit and similar levels at lower Lameta marls (Figs. 14, 15A). It is noted that this level of iridium is low by one to two orders of magnitude compared to levels reported from other KT boundary sections (Alvarez et al. 1980). The low value may indicate percolation of mobile iridium components through porous sands during diagenesis of boundary interval sediments.

Basu et al. (1988) briefly reported planar deformation features (PDF) in shocked quartz grains from the upper part of the KT boundary sandstone layer of Jabalpur using a petrographic microscope (Fig. 15B). This unit is characterized by a bimodal distribution of grain size with a dominant mode of medium-grained sand and a relatively minor mode of silt and clay frac-
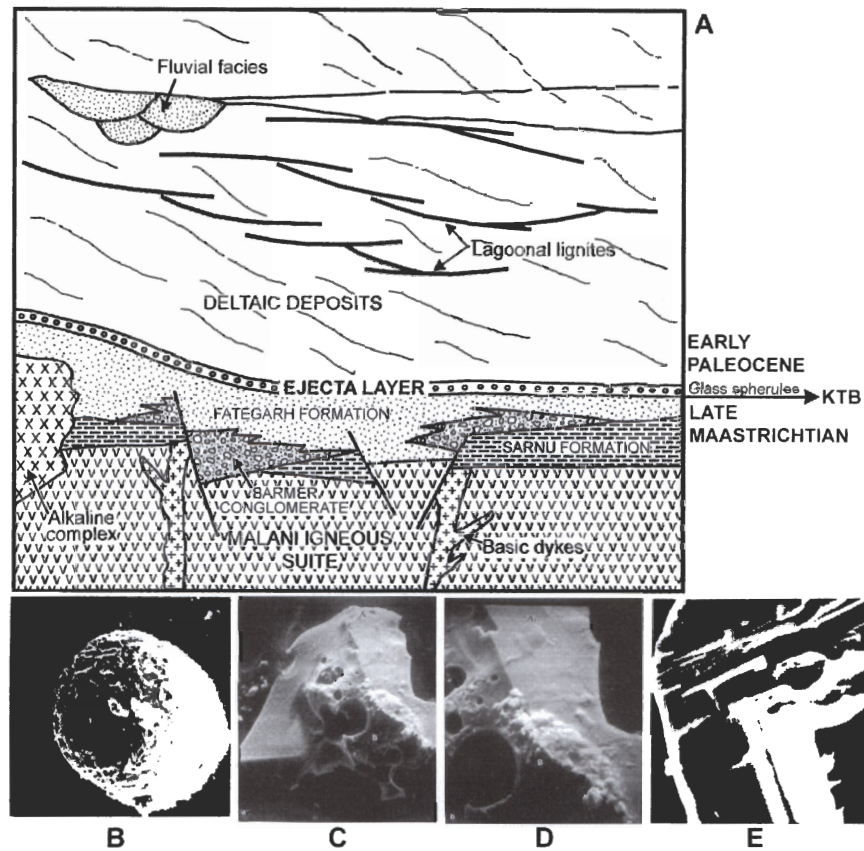
Figure 13. A, KT boundary section at Barmer, Rajasthan, showing the ejecta layer. B, scanning electron photographs of cosmic spheroid. C, vesicular glass. D, the same enlarged to show its Ni-rich region. E, skeletal structure of magnesioferrite spinel (simplified from Sisodia et al. 2005).
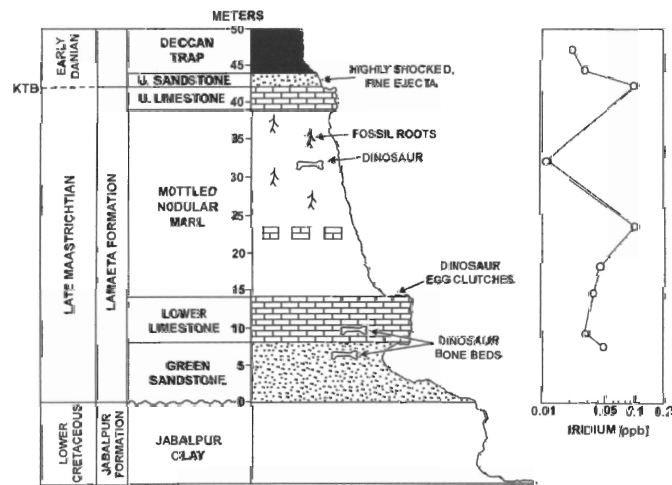

Figure 14. KT boundary section at Bara Simla Hill, Jabalpur, Madhya Pradesh, showing the stratigraphic position of the ejecta layer with shocked quartz below the Deccan lava flow; corresponding iridium profile on the right column (modified from Chatterjee 1992).
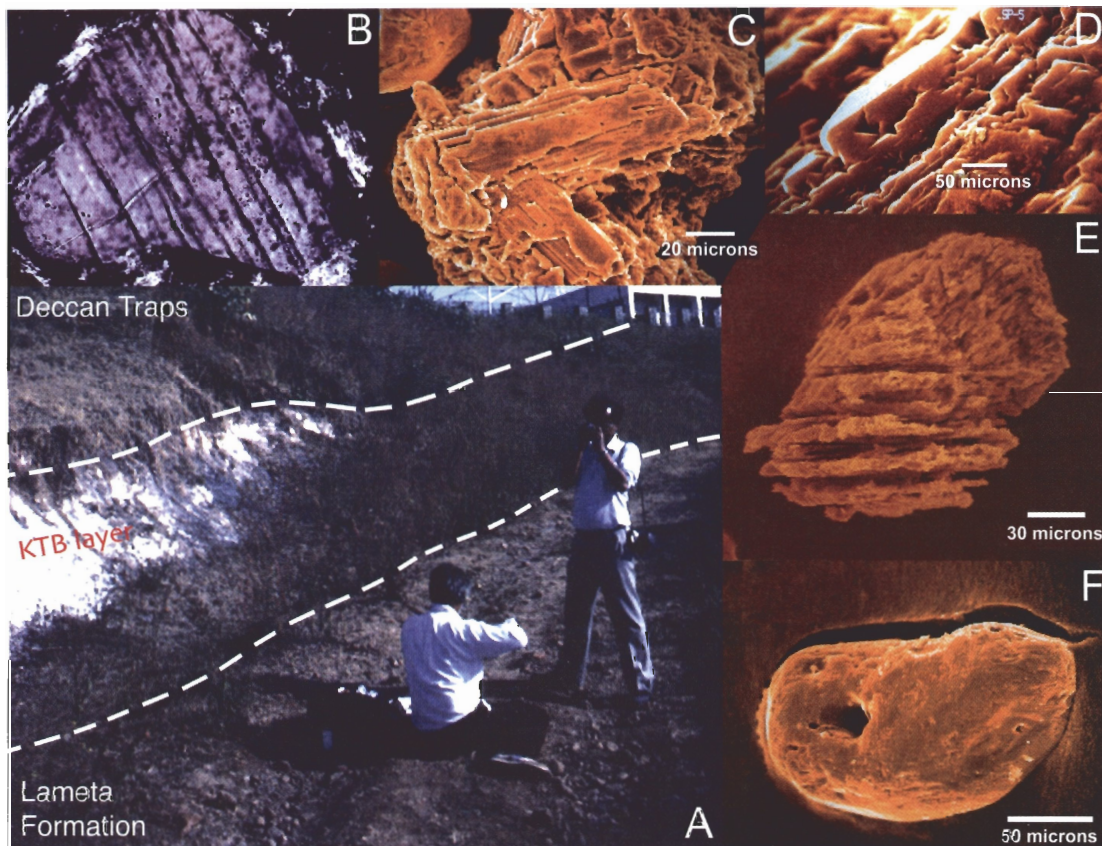
Figure 15. KT boundary ejecta layer at Bara Simla Hill, Jabalpur, Madhya Pradesh. A, stratigraphic position of the thick (~2.7 m) ejecta layer between Deccan Traps and Lameta Formation containing Late Maastrichtian dinosaur bones. B-E, shock-metamorphic features of quartz grains from the ejecta layer. B, quartz grain showing planar deformation features (PDF), which are decorated with fluid inclusions. The planes are closely spaced, numerous, straight and continuous throughout the grain. Some vitrification has also taken place along these planes. Long-dimension of the grain is 300 μm. Cross-polarized light. C-E, SEM photographs of shocked quartz grains from the ejecta layer showing three sets of planar deformation features etched with HF. Silica glass that partially filled the planar features has been etched out by the acid, leaving criss-cross pillars of a less soluble silica phase. F, a pure pellet of silica melt where the PDFs have been destroyed because of high shock pressure (> 60 GPa); the hole indicates the passage of the escaped vapor.

tions. The PDF-bearing quartz grains are relatively large (300 μm to 400 μm) that form about 2-3% of unetched samples and show many features commonly associated with impact. The planar features, both single and multiple, meet all criteria used to distinguish them from volcano-tectonic deformation (Bohor et al. 1987; Izett 1990). These criteria include well-defined sharp and straight features, which are parallel within a set, and continuous in multiple sets of narrow spacings extending across most of the grains (Fig. 15B). Quartz grains were mounted on a Universal Stage and PDF angles were measured (A. R. Basu, pers. comm.). The orientation of the poles to sets of planar features makes discrete angles with c-axis of quartz, with π and w being strongly prominent. These orientations are indicative of impact or shock-induced deformation. Mea-surements of 148 planar elements from 62 quartz grains show peak PDF concentration at about 23° to poles and about 32° to the optical c-axis of quartz grains, indicating PDF dislocations along the crystallographic planes w (1013) and π (1012) respectively and implying shock pressures over 16 GPa (Grieve

1990, 1996). Basu et al.'s (1985) observations provide convincing evidence of emplaced ejecta deposits immediately below the Deccan Traps.

Here we document further evidence of shock metamorphism of quartz grains from the upper sandstone unit of Jabalpur section by SEM images and Energy-dispersive X-ray spectra (EDXS). Clay-free mineral grains were prepared to determine their shock metamorphic effects. The residues consist primarily of silica, but also trace amounts of metallic particles. The mineral grains were immersed in 20% HF for 5 minutes and then coated with carbon and gold. SEM revealed the surface textures of the grains and EDXS showed their chemistries simultaneously. The X-ray spectra of the shocked minerals show pure silica composition with only Si- and O-lines. Quartz grains showing such multiple sets of shock-induced planar features are only found at meteoritic impact sites (Fig. 15C-E) as well as from other KT boundary sections (Bohor 1990; Bohor et al. 1987; Izett 1990). Usually in shocked quartz grains from the KT boundary, multiple sets of PDF are glass filled and therefore represent true shock deformation features (Bohor 1990). In many cases of Jabalpur samples, the acid has etched out silica glass that partially filled the planar features, leaving 'pillars' of less soluble silica phase (Fig. 15C-E). Most quartz grains shocked to ≥60 GPa melt completely and loose their crystalline structure altogether (Grieve 1990). We have recovered a dense phase of silica melt grain from the ejecta layer of the Jabalpur section, where the PDFs of quartz grain completely degenerated and turned into a glass spherule (Fig. 15F). We could not find any evidence of stishovite or coesite from the Jabalpur samples.

Shocked quartz grains from the Jabalpur section (300-400 μm) are coarse and relatively larger than most shocked quartz grain reported from Europe (100-200 μm) or the Pacific basin (< 100 μm) but somewhat smaller than those from North America (500-600 μm) (Bohor 1990; Bohor et al. 1987; Izett 1990). Of course, particles of this size scale still can be airborne over large distances, but the enormous thickness of the KT boundary section in Jabalpur favors the proximate source. Here, the KT boundary section appears to be very thick (2.7 m), possibly reworked, rather than a typical 1-cm thick deposit as in other KT boundary sites. This demonstrates the existence of a proximate

impact site such as the Shiva crater, from which thick distal ejecta could be emplaced ballistically. Such a thick boundary layer could not be derived as airborne fallout from the Chicxulub impact structure.

The absence of shocked quartz grains in other KT boundary sections of India is puzzling. We speculate that because of the giant Shiva impact (corresponding to shock pressures 100 GPa or more), the shocked quartz grains at the target rock must have been formed at the instant of impact but were quickly eradicated when the melt sheet formed. The absence of shocked quartz grains in other KT boundary sections implies that the bulk of the Shiva ejecta was melt, not moderately shocked quartz grains. It is important to note how little we know about large body impact products and how the products vary as a function of size, gravity, and velocity of bolide. Thus comparisons of impact products from a Chicxulub bolide may be poorly comparable to a Shiva-size bolide. There are many processes in nature when scaling larger not only produces larger effects, but produces new products of a different kind.

The clay fractions of the upper sandstone unit are of 90% smectite, which has been interpreted as the weathering product of a precursor glass or other silicate of impact material. Microtektites and glassy material resulting from an extraterrestrial impact has been offered as the possible parent material to the Jabalpur KT boundary clay (Schaef 1990) because structural formulas and chemical compositions of the Indian smectites are compatible with those from typical KT boundary clay layers, such as Stevens Klint of Denmark (Kastner et al. 1984).

Um Sohryngkew Section, Meghalaya.—The Um Sohryngkew river section of Meghalaya contains uninterrupted marine sequences of Cretaceous to Paleocene age that includes four successive formations from bottom to the top: Mahadeo, Langpur, Therria, and Lakadong (Fig. 16). The KT boundary layer, a 1.5 m cm thick limonitic layer based on planktonic foraminifera, lies within the Mahadeo Formation about 10 m below the Mahadeo/Langpur contact (Pandey 1990). This layer is rich in iridium, osmium and Ni-rich spinels (Fig.10D) (Bhandari et al. 1993, 1994; Robin et al., in press). The iridium profile at the KT boundary is about 12 ng/g, ten times higher than the
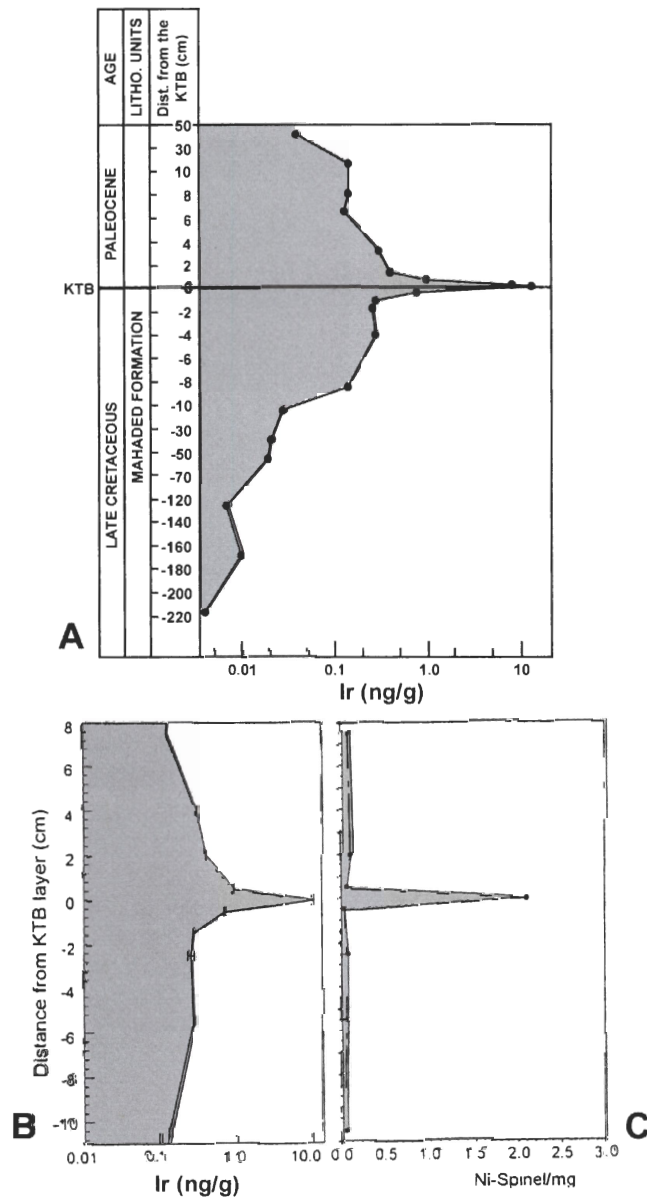
Figure 16. KT boundary section at Um Sohryngkew River section, Meghalaya. A, iridium anomaly at the KT boundary section depth profile. B, an expanded profile between -10 to +10 cm around KTB; meteoritic Ni-rich spinel spike at KTB (modified from Bhandari et al. 1994; Robin et al., in press).

background level. Ni-rich spinels in the Meghalaya section are almost absent below and above the KT boundary but show an abrupt increase in concentration with the maximum iridium spike. Ni-rich spinels are believed to have an unequivocal cosmic origin and have been reported from different KTB sections

(Robin et al. 1992). These spinels are characterized by magnesioferrite compositions with high concentrations of Ni and low Ti and Cr, which make them distinct from virtually all known terrestrial igneous or metamorphic occurrences. The number of spinels in the peak (2 spinels/mg) is, however, small as compared to

that found in most other KTB sections. Along with iridium and spinels, Bhandari et al. (2002) also reported cosmic magnetic nanoparticles from the KT boundary section of Meghalaya.

Ariyalur KTB Section, Tamil Nadu.—The KT boundary section at Anadavadi stream section, Ariyalur, Tamil Nadu, is composed of 16-m thick, coarse clastic marine deposits, indicative of high-energy deposition. Here the continental dinosaur-bearing Kallemedu Formation (Late Maastrichtian), equivalent to the Lameta Formation of Jabalpur, is overlain by the early Danian shallow marine Ninyur Formation (Fig. 17). The KT boundary age of the Ariyalur section is based on the paleontological evidence (Sahni et al. 1996). The Kallamedu Formation has yielded typical Late Maastrichtian palynological zone fossils such as *Aquillapollenites bengalensis*, whereas the overlying

Ninyur Formation has yielded typical early Danian nautiloids such as *Hercoglossa danica*.

A 1-m-thick oyster bed occurs at the contact with hummocky cross-stratifications with antiformal hummocks and synformal swales with dip angles and truncation angles of < 15°, as seen in the tsunami deposit at the KT boundary in Texas (Burgeois et al. 1988). Hummocky stratifications with shell fragments are generally interpreted as storm deposits. The oyster-bearing limestone is overlain by a 60-cm-thick concretion bearing sandy limestone, which in turn is overlain by 40-cm thick fine-grained sandstone. This sandstone unit includes small (<100 micron) spherules of carbonate that may be impact-generated (A. Glikson, pers. comm.). Madhavaraju et al. (2003) reported two types of distinctive magnetic susceptibility, C-zero and C4, from the sandstone unit (Fig. 17) that fits well
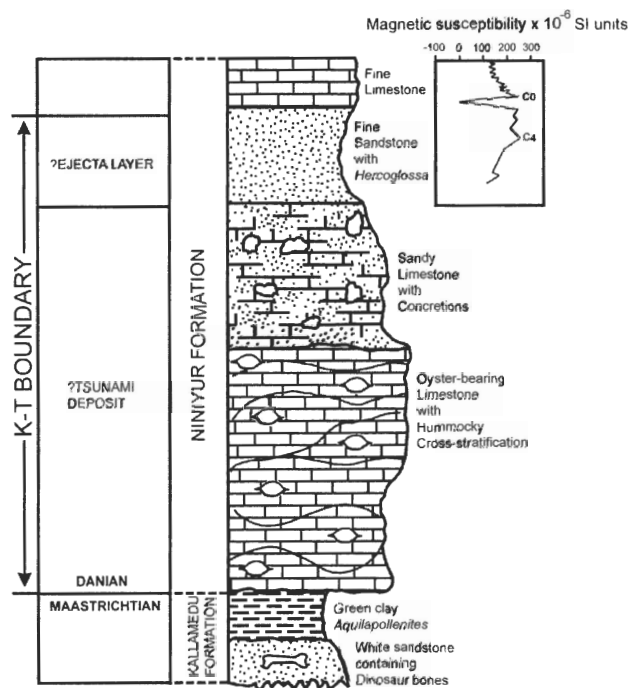

Figure 17. KT boundary section at Ariyalur, Tamil Nadu, showing 1.6 m-thick-tsunami deposits (?) with oyster bed showing characteristic hummocky stratification, followed by sandy limestone with concretions, and fine sandstone with possible ejecta components. From magnetic susceptibility analysis, the KT boundary appears to be at the top of the sandstone (modified from Madhavaraju et al. 2003).

with those of other KTB sections in the world corresponding to the 29R magnetic chron (Ellwood et al. 2003).

We interpret these 2-m thick coarse-grained beds to be the result of a major disturbance of the depositional environment such as a tsunami approximately 100 m high; the limestone bed, with oysters and sandy concretions, was ripped off from the shallow marine floor and dumped on the continental dinosaur-bearing Kallamedu Formation quickly by high-energy waves (Fig. 17).

Since the Shiva crater was located on the western shelf of India (Fig. 1), tsunami deposits should be expected to be more abundant on the west coast rather than on the east coast. However, thick lava piles of the Deccan Traps (> 2 km thick) form the Western Ghats Mountain range along the western coast that prevented any marine transgression at the KT boundary time. Thus the Deccan Trap Formation before the impact and its topography might have precluded the presence of abundant tsunami debris on the west coast. On the east coast of India, there was no such topo-

graphic barrier. This is possibly the reason for the tsunami deposits in the Ariyalur section of the east coast. Mehrotra et al. (2001) reported the presence of reworked Carboniferous palynofossils in the Paleocene Panna Formation in the Bombay High area, which is puzzling because Carboniferous sediments are not known from Peninsular India. But these palynofossils show affinity with those of Saudi Arabia and Africa across the Arabian Sea. They speculate that these palynofossils, entrapped within the sediments, might have been transported from the Saudi Arabia-Africa region by strong waves (tsunami?) and were deposited in the Bombay Offshore Basin in the Early Danian. If this scenario is correct, tsunami deposits should be investigated in the KT boundary sections of Saudi Arabia-Africa. Coffin and Rabinowitz (1986) mentioned massive tsunami deposits in the KT boundary section on the continental margin of Somalia and Kenya that encompasses an area of more than 20,000 km², with a minimum thickness of 1 km. These tsunami deposits on the western side of the Shiva crater may be linked to the Shiva impact.

SIZE AND TRAJECTORY OF THE SHIVA BOLIDE

Although hypervelocity impacts normally create circular craters, impacts at a low angle (~15° from the horizontal) often generate elongate craters such as Messier and Schiller craters on the Moon (Wilhelms 1987), Chicxulub crater in Mexico (Schultz and D'Hondt 1996), Shiva crater in India (Chatterjee and Rudra 1996), and the Rio Cuarto craters in Argentina (Schultz and Lianza 1992). Schultz and D'Hondt (1996) noticed several geophysical and morphological asymmetries in Chicxulub, where the crater rings are open to the northwest, like a horseshoe, which would be expected if the bolide came crashing in at angle of 20° to 30° from the southeast, digging a deep pit at the point where it landed and then continuing on a shallow path northwest.

Craters formed by artificial oblique impact are generally oblong (Gault and Wedekind 1978; Moore 1976). The shape of an artificial crater formed by oblique impact at 15° (Schultz and Gault 1990) is like a teardrop, where the pointed end indicates the downrange direction (Fig. 7B). In an oblique impact the

crater and its ejecta are bilaterally symmetrical about the plane of the trajectory, but the distribution of the ejecta is concentrated asymmetrically on the downrange side. The shape of the Shiva crater and the distribution of melt ejecta are almost identical to those produced by oblique impacts in laboratory experiments (Fig. 7). If the Shiva impact were the source of the alkaline igneous complexes, then this implies a significant asymmetry to the distribution of fluid ejecta. We suggest that the likely mechanism to generate this asymmetry would be a low-angle (< 30° from the horizontal) impact from southwest to northeast. This would provide a preferential direction for much of the fluid ejecta. If the Shiva projectile came from the southwest direction, the fluid ejecta would progress downrange with a mean direction of NE. If so, the impact that produced the Shiva crater was probably oblique along a SW-NE trajectory as evident from the distribution of the longer diameter of the oblong crater; the tip of teardrop indicates that the downrange direction was NE. Howard and Wilshire (1975) described flows of impact melt of large lunar craters both outside on

crater rims and inside on the crater walls, where asymmetric distribution of fluid ejecta can be used to determine the impact trajectory. The asymmetric distribution of fluid ejecta on the NE side of the Shiva crater indicates the downrange direction. A low-angle impact from the southwest is consistent with the asymmetry of seismic, geothermal, and gravity anomalies at the Mumbai coast (Fig. 9).

The distribution of KT boundary ejecta in the NE direction of the Shiva crater is consistent with the trajectory of the bolide. Moreover, the enormous strewnfield of magnesioferrite spinel distribution, along with shocked quartz in KT boundary sediments of the Pacific basin, lie directly on this northeast trajectory (Kyte and Bostwick 1995) of the Shiva bolide. These authors noticed that composition of these cosmic spinels from the Pacific is markedly different from those found in western Europe and the South Atlantic. We believe the compositional variations of cosmic spinels in KT boundaries indicate two impact sources:

Chicxulub structure for the European and Atlantic distribution and the Shiva structure for the source of the Pacific impact debris. As the vapor cloud would progress downrange from the Shiva structure toward the Pacific, the earliest and highest temperature phases would drop as airborne particles, first at Meghalaya and then over the Pacific (Fig. 18).

Wetherill and Shoemaker (1982) summarized the current knowledge of Earth-crossing and Earth-orbiting asteroids. They listed three large asteroids that exceed 10-km in diameter: Sisyphus (~11 km), Eros (~20 km), and Ganymed (~40 km). Using the crater scaling method (Grieve and Cintala 1992), we estimate that a 40-km diameter asteroid (having a mass of 10^{16} kg) about the size of Ganymed, striking at a speed of 15 km/s, could have created the Shiva crater with a 500 km diameter and ~10^6 km^3 of impact melt produced by three distinct stages (Elkins-Tanton and Hager 2005), as discussed earlier.
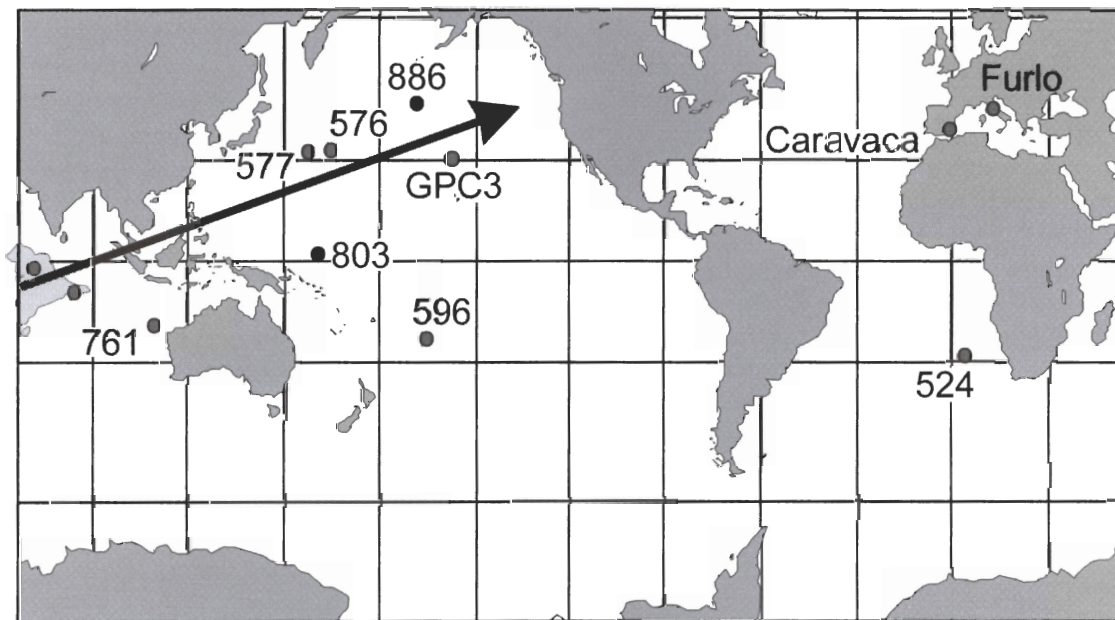

Figure 18. Distribution of KT boundary magnesioferrite spinel in the Pacific basin that lies along the trajectory of the Shiva bolide. These spinels might be derived from the Shiva impact site (modified from Kyte and Bostwick 1995).

GEODYNAMIC CONSEQUENCES OF THE SHIVA IMPACT

The impact of a large bolide into the Earth may have set in motion a very complex array of events with intriguing consequences. For typical terrestrial impact velocities of 15-25 km/s, the impacting body penetrates the target rock approximately 2-3 times its radius and transfers most of its kinetic energy to the target (Grieve 1987). Impact of the bolide may have produced a vast transient crater 50 km deep and 250 km across, which quickly collapsed under the force of the gravity, leaving a basin 500 km wide and 7 km deep. The energy from the 10-km-diameter Chicxulub bolide is estimated to be about 10^{24} Joules, equivalent to the explosion of 100 trillion tons of TNT, or about 10,000 times greater than the explosive energy of the world's entire nuclear arsenal (Frankel 1999; Grieve 1990). If so, the Shiva bolide (~40 km diameter) would generate so much energy that it could create isostatic instability leading to uplift, possibly resulting in shattering of the lithosphere, rifting, volcanism, and other rearrangement of the interior dynamics of the planet. Thus, the Shiva impact not only created the largest crater on Earth, but also initiated several other geodynamic anomalies. Some authors have suggested relationships between large impacts and phenomena such as magnetic reversals and plate movements (Clube and Napier 1982), but these suggestions remain unproven. The Shiva provides for the first time tangible evidence linking large impact with seafloor spreading and evolution and jumping of nearby spreading ridges. It appears that both the Shiva impact and adjacent spreading centers such as the Carlsberg Ridge and Laxmi Ridge are part of a single thermal system. The Shiva impact produced cratering and associated tectonic rebound/collapse effects sufficient to locally disrupt the entire lithosphere and cause a major change in plate stress patterns such that stress would propagate quite rapidly away from the immediate region of the impact. It caused major changes in the Indian plate motion and lithospheric stress patterns. The impact might have important consequences on the evolution and propagation of nearby spreading ridges around the Shiva crater in the northwestern Indian Ocean. Whereas Late Cretaceous magnetic lineations in other oceans show no obvious signs of disturbances at the Tertiary boundary, the end-Cretaceous Indian plate boundary in the Indian Ocean provides evidence of major tectonic reorganization at or shortly after

magnetostratigraphic chron 29R that might be linked to the Shiva impact. The effects of major plate tectonic changes at about chron 29R, when the Seychelles rifted from India, were not confined to the northwestern Indian Ocean; they are also observed over an extensive segment of former African plate boundary in the southwestern Indian and Southern Atlantic oceans, involving both the Antarctic and South American plates. In the Agulthus Basin, a westward ridge jump of more than 800 km occurred at the KT boundary time between the African and South American plates (Hartnady 1986).

India-Seychelles Rifting.—A new rift between Indo-Somalia and Seychelles was formed near the KT boundary (65 Ma) coinciding with the Shiva impact (Chatterjee and Scotese 1999). At this time the Central Indian Ridge (CIR) jumped 500 km northward from its location in the Madagascar Basin to a new location between the Seychelles and Indo-Somalia to form the Carlsberg Ridge. The Mascarene basin spreading center became extinct as a possible response of this emplacement. This ridge jump (>500 km) caused a sliver of continent to split off from Indo-Greater Somalia, forming the Seychelles microcontinent. It resulted in sudden transfer of the Seychelles and Mascarene bank to the African plate (Fig. 19). This ridge jump may be linked to the Shiva impact on the trailing edge of the Indo-Seychelles block (Hartnady 1986). This impact may have formed a large lithospheric crack between India and Seychelles and initiated the creation of the Carlsberg Ridge, triggering readjustments along the Indian-African and Antarctic-African plate boundaries (Chatterjee and Rudra 1996; Hartnady 1986). Hartnady (1986) speculates that anomaly 29 may appear near the base of the steep microcontinental slope of Seychelles. If these identifications are correct, then rifting occurred just before chron 29 and may correspond to chron 29R (KT boundary). At present, there is a time lag (~2 Ma) between the impact (29R) and its subsequent expression in chron 28R of the rifting of the Carlsberg Ridge.

Westward Jump of the Spreading Ridge of the Laxmi Basin.—The Laxmi Ridge, an enigmatic continental sliver in the Arabian Sea, about 700 km long and
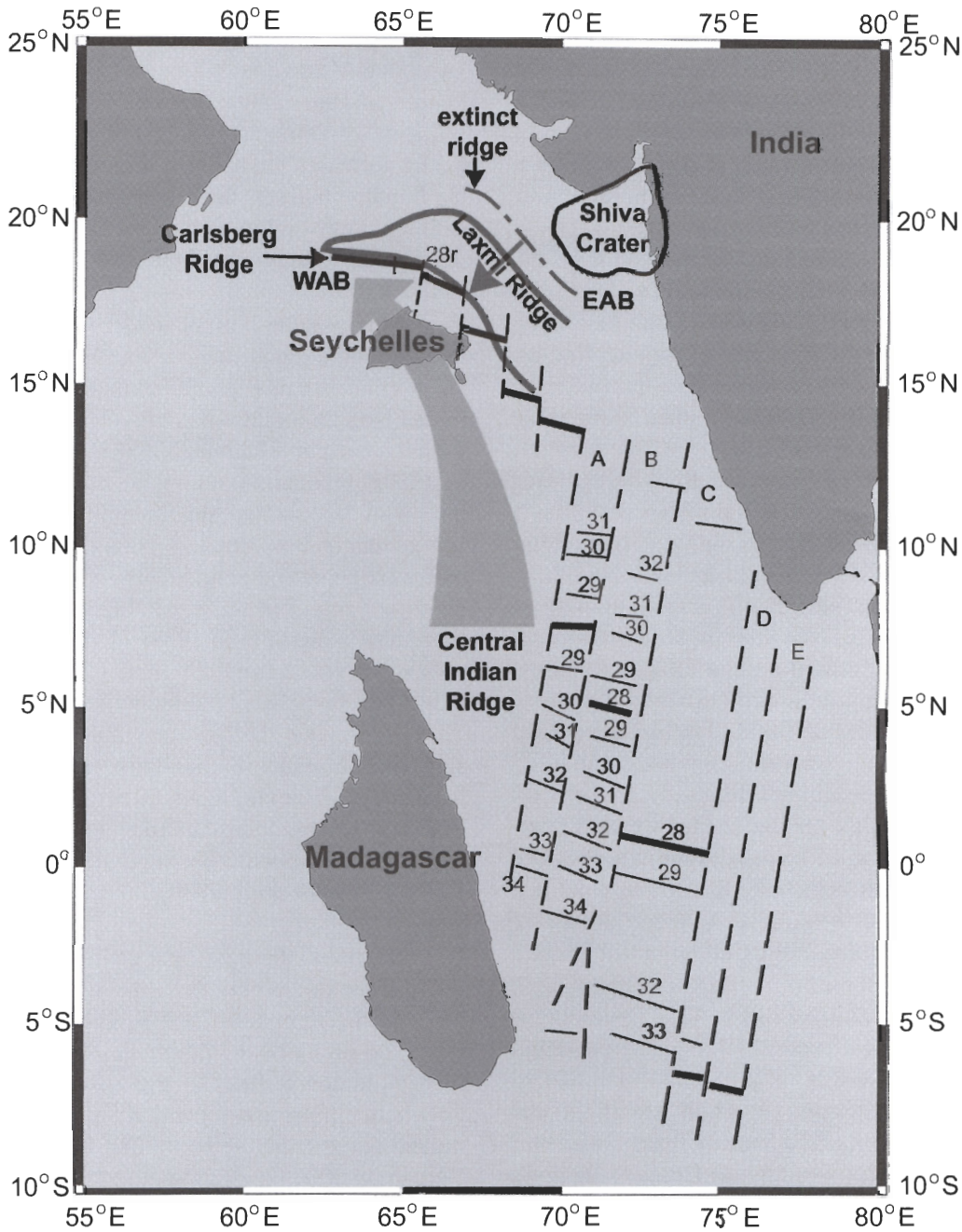
Figure 19. KT boundary plate reconstruction showing the paleopositions of India, Laxmi Ridge, Seychelles, and Madagascar. During the Shiva impact, there was plate reorganization in the northwest Indian Ocean when the Central Indian Ridge jumped more than 500 km northward to form the Carlsberg Ridge, thus initiating the rifting between India and Seychelles. At the same time an extinct ridge in the East Arabian Basin (EAB) between Laxmi Ridge and the Shiva crater jumped 500 km westerly to West Arabian Basin (WAB) between Seychelles and Laxmi Ridge. A-E represent different fracture zones (modified from Hartnady 1986; Talwani and Reif 1998; Dyment 1998).

100 km across, occurs west of the Shiva crater (Figs. 3, 19). Although the origin of Laxmi Ridge is still controversial, gravity and seismic data indicate that it is quite different from a typical oceanic ridge and is probably continental in origin (Dyment 1998; Talwani and Reif 1998). It formed two basins, one on each side: the East Arabian Basin (EAB) and the West Arabian Basin (WAB). In the East Arabian Basin, a short duration of seafloor spreading commenced from the A28-A33 interval of geomagnetic chron, which finally ceased around 65 Ma (Bhattacharya et al. 1994). At the same time, with the extinction of the East Arabian Basin spreading center, the ridge suddenly jumped more than 500 km westerly to the West Arabian Basin on the other side of the Laxmi Ridge, as a possible response to the Shiva impact (Talwani and Reif 1998). This ridge jump is synchronous with the Mascarene Basin jump of the Carlsberg Ridge. In the West Arabian Basin, regular sea-floor spreading anomalies have been identified; the oldest anomaly was chron 28R. Apparently, the opening of the East Arabian Basin commenced around 84 Ma and ceased around 65 Ma, when the spreading center jumped from east to west of the Laxmi Ridge to the West Arabian Basin. The age relationship between the Shiva impact and the cessation and westerly jump of the spreading of the Laxmi Ridge is intriguing. We speculate that the sudden westerly jump of the Laxmi Ridge at KT boundary time may be linked to the Shiva impact, which readjusted the plate tectonic framework of the Arabian seafloor coinciding with the northerly jump of the Central Indian Ridge.

Origin of the Deccan Traps.—The Deccan traps are one of the largest continental volcanic provinces of the world. It consists of more than 2 km of flat-lying basalt lava flows and covers an area of 500,000 km^2, roughly the size of the State of Texas. Estimates of the original area covered by the Deccan lava flows including the Seychelles-Saya De Malha Bank are as high as 1,500,000 km^2 (White and McKenzie 1989). The Deccan traps are flood basalts similar to the Columbia River basalts of the northwestern United States, formed by the Yellowstone hotspot.

Currently three models for the origin of the Deccan basalt volcanism have been proposed: mantle plume theory, plate rift theory, and impact-induced theory. In mantle plume theory, Deccan flood basalts were the first manifestation of the Reunion hotspot

that rose from the core-mantle boundary and subsequently produced the hotspot trails underlying the Laccadive, Maldive, and Chagos islands; the Mascarene Plateau; and the youngest volcanic islands of Mauritius and Reunion (Morgan 1981). The age of the hotspot tracks decreases gradually from the Deccan traps to the Reunion hotspot, thus appearing to be consistent with the northward motion of the Indian plate over a fixed plume (Duncan and Pyle 1988).

Although the hotspot model is very attractive, there are some geochemical problems with this model. Geochemical analysis indicates that the likely source for the Deccan volcanism is rift volcanism rather than Reunion hotspot (Mahoney 1988). Later, Mahoney et al. (2002) recognized several phases of non-MORB phases of Deccan volcanism. Further geochemical and geothermal evidence suggests that Deccan magmas were generated at relatively shallow (34-45 km) depth and rules out the possibility of its origin by a deep mantle plume (Sen 1988). To circumvent these criticisms, White and McKenzie (1989) proposed a model that combines both plume and rifting origins. They argued that the Deccan volcanism was associated with the breakup of the Seychelles microcontinent from India. The enormous Deccan flood basalts of India and the Seychelles-Saya de Malha volcanic province were created when the Seychelles split above the Reunion hotspot (Figs. 7, 10).

However, there is some conflict of timing between these two events: the onset of Deccan volcanism and rifting of India and Seychelles. What triggered the rifting of the Seychelles from India? Was it the Reunion hotspot or the Shiva impact? The Carlsberg rifting that separated Seychelles from India did not start before chron 28R (63 Ma), whereas Deccan volcanism started somewhat earlier around 30N (66 Ma) (Fig. 11). Thus the Deccan volcanism predates the India-Seychelles rifting event, making the causal link unlikely (Chatterjee and Rudra 1996).

A third view for the origin of the Deccan Traps is the impact-triggered model. The spatial and temporal coincidence of Deccan volcanism with the Shiva crater led to the suggestion that the Deccan Traps might mark the site of the asteroid impact (Alt et al. 1988; Alvarez and Asaro 1990; Basu et al. 1988; Hartnady 1986). Although the idea of genetic association be-

tween impact and volcanism is very appealing, especially from cratering studies of the Moon where impacts caused lava to fill the crater basins (lunar maria), it is rejected because of conflict of timing; the slow outpouring of Deccan volcanism preceded the KT impact by 400 Kyr or more (Fig. 11). Thus, impact cannot be the proximate cause for the initiation of the Deccan volcanism (Bhandari et al. 1995; Chatterjee and Rudra 1996). However, impact could enhance the volcanic activity by decompression melting beneath the impact site (Jones et al. 2002; Elkins-Tanton and Hager 2005). At the KT boundary (65 Ma), the trickle of Deccan lava eruption became a torrent as is evident from the thick pile of lavas; seismic shock waves from the Shiva impact might have galvanized the proximate Deccan-Reunion hotspot and induced spectacular burgeoning of the Tertiary Deccan volcanism by rifting India and Seychelles (Fig. 10). An impact of this magnitude could raise the crust-mantle boundary close to the surface by decompression, as seen in the western coast of India, and create a large volume magma chamber (Fig. 9). Jones et al. (2002) proposed a mechanism to explain how a major impact could trigger large-scale volcanism, such as the Siberian Traps at the end of the Permian, by decompression melting of the lithosphere. Thus, the Shiva impact might be indirectly responsible for rapid and spectacular areal distribution of the Deccan lava piles during its waxing stage. Sen (1988) noticed that continental lithosphere was involved in the melting and contamination process during the generation of the Deccan lava. Perhaps impact rather than the plume was the cause of the lithosphere melting during the KT boundary eruption. Although the close temporal coincidence between the Shiva crater and the Reunion hotspot that created the Deccan volcanism is statistically an unusual event, it is not entirely impossible; the modern analogy would be a large bolide striking close to the Yellowstone hotspot, Kilauea, Reunion, Kerguelen islands, or near any of the numerous active hotspots.

The pre-KT Chicxulub impact nearly coincides with first phase of the Deccan volcanism (Keller et al. 2003). Is there any causal link between these two events, which are located almost in antipodal positions? Impact-induced antipodal volcanisms are suggested from Mars. An alternative view, which involves Chicxulub impact but not an in-situ strike, maintains that lithospheric fracturing and Deccan flood basalt

volcanism could be triggered by the transmission and focusing of shock waves from a major antipodal impact (Boslough et al. 1996). Thus, Deccan volcanism could reflect a Chicxulub impact, although cause and effect would be offset by 120° rather than 180° (Sutherland 1996). However, oblique impact at the Chicxulub may account for this antipodal discrepancy.

Northward Acceleration of the Indian Plate.— During most of the Mesozoic, the Indian plate moved northward at a rate of 3-5 cm/year. The sudden acceleration of the Indian plate to the super fast rate of 15-20 cm/year from Late Cretaceous (80 Ma) to Paleocene (53 Ma) time has long been a major puzzle in plate tectonics and has provoked many speculations (Patriat and Achache 1984). This faster rate was sustained for about 20 My during the Paleocene, soon after the KT impact, and then slowed down as the Indian plate began to plow into the Eurasian continent. Negi et al. (1986) suggested from heat flow data that the Indian lithosphere was greatly thinned (about one third of that of other global shields), abnormally hot, and lighter during this period, which had important consequences for mantle rheology. It reduced the drag of the lithosphere against the asthenosphere, resulting in faster northward movement of the Indian plate. Apparently the Indian plate decoupled itself from the deeper interior to become more mobile. We speculate that the acceleration of the Indian plate may be linked to the India-Seychelles rift at the KT boundary with the initiation of the Carlsberg Ridge. During the Paleocene, the Indian plate slowed its northward motion from about 20 cm/year to 4.5 cm/year as it collided with Asia (Chatterjee and Scotese 1999).

As discussed earlier, the Shiva impact might cause thermal erosion of the lithosphere, and, thereby, produce a thinned lithosphere and high heat flow (Pandey and Agarwal 2001). The sudden northward acceleration of the Indian plate during the KT boundary time might also be linked to the oblique impact of the 40-km diameter Shiva bolide at a speed of 15-25 km/s in a northeast direction that generated a vast amount of tangential kinetic energy at the striking point. The impactor-driven force would have pushed the thin, hot and mobile Indian plate farther northward, creating a spreading asymmetry. Dyment (1998) noticed that during anomalies 26 and 25, about 65% of the crust formed at the Carlsberg Ridge was accreted to

the African plate, while at anomalies 24-20, more than 75% benefited to the Indian plate. We speculate that these asymmetries result from the relative position of the Carlsberg Ridge and nearby Shiva impact, the ridge tending to remain near the crater. A unique aspect of the Indian plate at that time was its fast velocity, which moved northward from an almost stationary Antarctica. The asymmetric spreading of the Indian plate, resulting from the ridge propagation along the Carlsberg Ridge, may be related to the oblique impact of the Shiva bolide.

PETROLEUM ENTRAPMENT

KT boundary impact craters such as Shiva, Chicxulub, and the Boltysh depressions are among the most productive hydrocarbon sites on Earth. Donofrio (1981, 1998) recorded 17 confirmed impact structures/events occurring in petroliferous areas of North America, nine of which are being exploited for commercial hydrocarbons. Interestingly, all craters containing commercial oil and gas were accidental discoveries. They yield from 30 to over 2 million barrels of oil per day plus over 1.5 billion cubic feet of gas per day. The impact cratering process results in unique structures and extensive fracturing and brecciation of the target rock, which can be conducive to hydrocarbon accumulations. Reservoirs are found in sedimentary and crystalline basement rock and usually consist of central uplifts, rims, slump terraces, and ejecta and probably subcrater fracture zones (Fig. 20). Additionally, sediments overlying an impact structure can form numerous structural and stratigraphic traps, such as anticlines and pinchouts, which can be enhanced during crater isostacy.

In the Chicxulub crater, the impact products such as carbonate breccia forms the reservoir rocks, whereas the overlying dolomitized ejecta layer forms the seal (Grajales-Nishimura et al. 2000). Chicxulub reservoirs are most likely tsunami formed and are found in post-impact structural traps about 140 km—within two crater radii—southwest of the rim in the offshore bay of Campeche. Estimated reserves for the Chicxulub event are ~30 billon barrels of oil and 12 trillion cubic feet of gas.

In the Shiva crater, the most prolific traps are those located on persistent paleo-highs of the peak ring area, where oil and gas is produced primarily from Middle Miocene reservoirs, with the most prolific being the platform carbonates such as the Lower Mi-
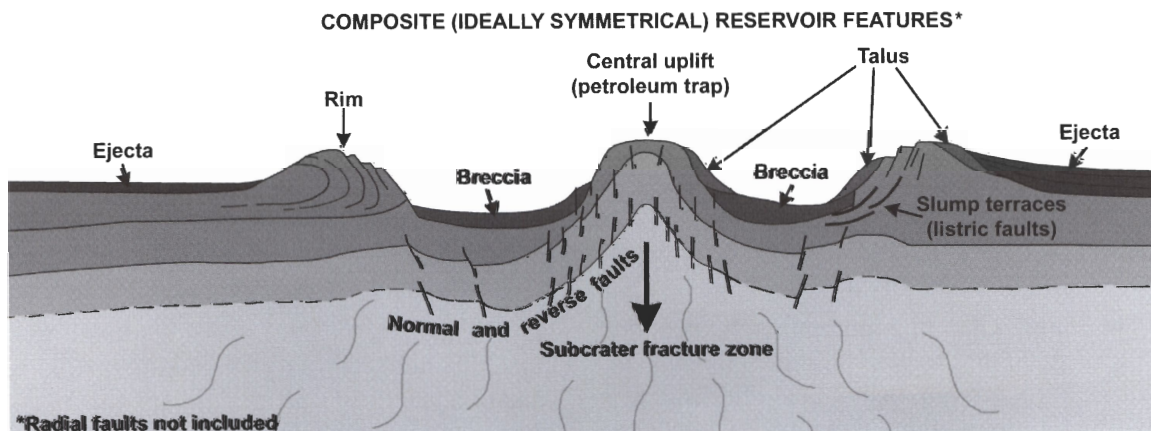

Figure 20. Diagrammatic cross-section of a complex impact crater showing how the central uplift and other shattered units may be effective petroleum trap. All the KT boundary impact craters, such as Chicxulub, Shiva, and Boltysh, have central peaks and are excellent structural traps for giant oil and gas fields.

ocene Ratnagiri Formation (Rao and Talukdar 1980). Fractured basement rock also has hydrocarbon potential. The most likely seals are an extensive series of thick middle to Upper Miocene shales. Ranked 38th worldwide, Shiva has reserves exceeding 8.4 billion barrels of oil, 24.2 trillion cubic feet of gas, and 0.3 billion barrels of natural gas liquids (Wandrey 2004). The total 12.7 billion barrels of oil equivalent including natural gas liquids, is from 165 fields of which 126 are one million barrels of oil equivalent or greater in size (Petroconsultants 1996).

The Boltysh impact crater in the Ukraine is a circular depression about 24-km in diameter formed in crystalline basement rocks (Kelley and Gurov 2002). But while Chicxulub and Shiva filled with seawater, the Boltysh crater became a freshwater lake. The annular trough surrounds the central uplift, which is about 580 m in height and 4 km in diameter. The Boltysh structure is filled with post-crater sediments of argillites and siltstones. Commercial reserves of oil shales (sapropelites) occur in sedimentary crater fill, which constitute about three billion tons (Yurk et al. 1975). When processed, these oil shales could yield several billion barrels of oil.

BIOTIC CONSEQUENCES

At the close of the Cretaceous, the Earth was devastated. Life was ravaged by one of the worst catastrophes. Of all five major extinctions that happened during the Phanerozoic, the KT extinction has captured the most public attention, because of the demise of dinosaurs. The dinosaurs dominated the landscape more than 160 My, living over a thousand times longer than the tenure of modern humans (*Homo sapiens* first evolved around 150 Kya). After more than two decades of debates, the proximate cause for the KT extinction still remains controversial. There are two competing models: bolide impact (Alvarez et al. 1980) or flood basalt volcanism (Courtillot 1990; Officer et al. 1987). Three Phanerozoic mass extinctions are now reported to be linked temporarily with both volcanism and impacts (White and Saunders 2005): the Permo-Triassic (P-Tr, 250 Ma), the Triassic-Jurassic (Tr-J, 200 Ma), and the KT extinction (65 Ma). Another major unresolved factor in the KTB impact story is the exact number of impacts involved (Glen 1990, 1994). Three impacts, Chicxulub, Boltysh, and Shiva are known to have occurred at the KT transition, spaced over an interval of time of approximately 300,000 years (Keller et al. 2003, 2004), and are supported by the presence of multiple layers of iridium and fullerene anomalies in the Anjar section of Gujrat (Parthasarathy et al. 2002).

The Boltysh impact was relatively small, affecting the local areas on the Ukranian shield with little global influence. However, it probably occurred around the same time as Shiva. The Chicxulub crater appears to have been formed 300 Kyr before the KT boundary and cannot be the proximate cause for the end-Cretaceous mass extinction (Keller et al. 2004). A single large meteorite impact like the Shiva may be more harmful to life than a cluster of several smaller meteorites spread over 300 Kyr. However, the Chicxulub impact coincided with the early phase of the Deccan volcanism, and those two processes may have created high stress environments causing a gradual decrease of species diversity during the last 300 Kyr before the KT boundary. Chatterjee and Rudra (1996) argued that although Deccan volcanism injected 10 times more CO_2 into the atmosphere to increase the greenhouse effect, reduce photosynthesis, create acidic oceans, dissolve shells of calcareous organisms, and collapse the marine food chain, Deccan volcanism could not be the proximate cause of the KT extinction, because dinosaur bones and their eggs have been found in intertrappean beds interlayered with Deccan lava flows (Fig. 11). Dinosaurs were thriving in India when Deccan lava was erupting. The kill mechanisms associated with Deccan volcanism were slow and gradual and do not appear to be sufficiently powerful to cause worldwide collapse of ecosystems suddenly at the KT boundary leading to the one of the largest mass extinctions. Thus, the influence of Deccan lavas for the biotic crisis is indirect, perhaps through greenhouse warming generated by the injection of large amounts of CO_2 into the atmosphere and the change of the ocean chemistry by production of acid rain.

Elimination of Chicxulub, the Boltysh impacts, and Deccan volcanism from the extinction equation leaves the Shiva impact as the sole candidate for the final blow to the apocalyptic disaster at the KT boundary, which claimed dinosaurs, pterosaurs, plesiosaurs, mosasaurs, rudists, ammonites, and more than 75% of animal and plant species on Earth. The pressure exerted by the Shiva impact could have exceeded 100 GPa; temperatures could have reached several thousand degrees Celsius; and impact energy would have generated more than a 100-million megaton blast (Grieve 1990). The biologic consequences of such a huge impact, which were nearly instantaneous in their globally devastating effects, would have depended on many factors, including the energy of the impact event, the type and location of target materials, the type of projectiles, and the prevailing ecology. While the greatest damage is obviously at ground zero for a large impact, a very significant portion of the energy from the impact would have been dissipated and devastated the ecosphere, the thin shell of air, water, soils, and surface rocks that nurture life, and cause the mass extinction. Even seismic shock waves would reach damaging proportions on a global scale and would trigger tsunami that would flood most shorelines ~100 km inward and destroy coastal life (Chapman 2002). The trajectory of the Shiva bolide should have driven a fiery vapor cloud toward the northeast, creating a corridor of incineration across east-central India that would reach the Pacific Ocean (Fig. 18). Although the most extreme devastation was to the northeast of the Shiva crater, lethal consequences encompassed the entire globe at different tempos. Accumulating evidence suggests that the extinctions were uneven in a global context (Sutherland 1996). Many authors (Alvarez et al. 1980; Anders et al. 1991; Toon et al. 1997) have examined specific aspects of environmental stresses following a large impact. Chatterjee and Rudra (1996) reviewed various models of impact-generated environmental changes and killing mechanisms such as shock wave, global fire, perpetual night resulting from ejecta dust particles that would screen out nearly all sunlight and halt photosynthesis, collapse of the food chain, ozone layer destruction, toxicity of the environment, acid trauma, nuclear winter, and earthquakes and tsunamis at the KT boundary. The climatic calamity decimated flora and fauna globally. Recently Robertson et al. (2004) proposed that an infrared thermal pulse from a global rain of hot spherules splashed from the KT impact was the primary killing agent. According to this model, for several hours following the impact, the entire Earth was scorched with infrared radiation from reentering ejecta that would have killed unsheltered organisms directly and ignited global fires that consumed Earth's forests and their dwellers.

LITERATURE CITED

Alt, D., J. M. Sears, and D. W. Hyndman. 1988. Terrestrial maria: the origins of large basal plateaus, hotspot tracks, and spreading ridges. Journal of Geology 96:647-662.

Alvarez, L. W., W. Alvarez, F. Asaro, and H. V. Michel. 1980. Extraterrestrial cause for the Cretaceous-Tertiary extinction. Science 208:1095-1108.

Alvarez, W., and F. Asaro. 1990. An extraterrestrial impact. Scientific American 263:78-84.

Anders, E., W. S. Wolbach, and I. Gilmore. 1991. Major wildfires at the Cretaceous-Tertiary boundary. Pp 485-492 in Global biomass burning: atmospheric, climatic, and biospheric implications (J. S. Levine, ed.). Massachusetts Institute of Technology Press, Cambridge, Massachusetts.

Baker, B. H. 1967. The Precambrian of the Seychelles Archipelago. Pp 122-132 in Precambrian research (K. Rankama, ed.). Interscience, New York, New York.

Basu, A. R., S. Chatterjee, and D. Rudra, 1988. Shock-metamorphism in quartz grains at the base of the Deccan Traps: evidence for impact-triggered flood basalt volcanism at the Cretaceous-Tertiary boundary. EOS (Transactions, American Geophysical Union) 69:1487.

Basu A. R., P. R. Renne, D. K. Das Gupta, F. Teichmann, and R. J. Poreda. 1993. Early and late alkali igneous pulses and a high - ³He plume origin for the Deccan Flood Basalts. Science 261:902-906.

Basu, D. N., A. Banerjee, and D. M. Tamhane. 1982. Facies distribution and petroleum geology of Bombay Offshore Basin, India. Journal of Petroleum Geology 5:57-75.

Becker, L., J. L. Bada, R. E. Winans, J. E. Hunt, T. E. Bunch, and B. M. French. 1994. Fullerenes in the 1.85 billion year old Sudbury impact structure. Science 265:642-645.

Berggren, W. A., D. V. Kent, J. J. Flynn, and J. A. Van Couvering. 1985. Cenozoic geochronology. Geological Society of America Bulletin 96:1407-1418.

Bhandari, L. L., and S. K. Jain. 1984. Reservoir geology and its role in the development of the L-III reservoir, Bombay High Field, India. Journal of Petroleum Geology 7:27-46.

Bhandari, N., P. N. Shukla, Z. G. Ghevariya, and S. M. Sundaram. 1995. Impact did not trigger Deccan volcanism: evidence from Anjar K/T boundary intertrappean sediments. Geophysical Research Letters 22:433-436.

Bhandari, N., P. N. Shukla, Z. G. Ghevariya, and S. M. Sundaram. 1996. K/T boundary layer in the Deccan intertrappeans at Anjar Kutch. Geological Society of America Special Paper 307:417-424.

Bhandari, N., H. C. Verma, C. Upadhyay, A. Tripathi, and R. P. Tripathi. 2002. Global occurrence of magnetic and superparamagnetic iron phases in Cretaceous-Tertiary boundary clays. Geological Society of America Special Paper 356:201-211.

Bhattacharya, G. C., A. K. Chaubey, G. P. S. Murthy, K. Srinivas, K. V. L. N. S. Sarma, V. Subrahmanyam, and K. S. Krishna. 1994. Evidence for seafloor spreading in the Laxmi basin, northeastern Arabian Sea. Earth and Planetary Science Letters 125:211-220.

Biswas, S. K. 1987. Regional tectonic framework, structure and evolution of the western marginal basins of India. Tectonophysics 135:305-327.

Blum, J. D., C. P. Chamberlain, M. P. Hingston, C. Koeberl, L. E. Martin, B. C. Schuraytz, and V. L. Sharpton. 1993. Isotopic comparison of K/T boundary impact glasses with melt rock from the Chicxulub and Manson impact structures. Nature 364:325-327.

Bohor, B. F. 1990. Shocked quartz and more: impact signatures in Cretaceous/Tertiary boundary clays. Geological Society of America Special Paper 247:335-342.

Bohor, B. F., P. J. Modreski, and E. E. Foord. 1984. Shocked quartz in the Cretaceous-Tertiary boundary clays: evidence for a global distribution. Science 224:705-709.

Bose, M. K. 1980. Alkaline magmatism in the Deccan volcanic province. Journal of the Geological Society of India 21:317-329.

Boslough, M. B., E. P. Chael, T. G. Trucano, D. A. Crawford, and D. L. Campbell. 1996. Axial focusing of impact energy in the Earth's interior: a possible link to flood basalts and hotspots. Geological Society of America Special Paper 307:541-550.

Bourgeois, J., T. A. Hansen, P. L. Wiberg, and E. G. Kauffman. 1988. A tsunami deposit at the Cretaceous-Tertiary boundary in Texas. Science 241:567-569.

Chapman, C. R. 2002. Impact lethality and risk in today's world: lessons for interpreting Earth history. Geological Society of America Special Paper 356:7-19.

Chatterjee, S. 1992. A kinematic model for the evolution of the Indian plate since the Late Jurassic. Pp. 33-62 in New concepts in global tectonics (S. Chatterjee and N. Hotton, eds.). Texas Tech University Press, Lubbock, Texas.

Chatterjee, S. 1997. Multiple impacts at the KT boundary and the death of the dinosaurs. Proceedings of the 30th International Geological Congress 26:31-54.

Chatterjee, S., N. Guven, A. Yoshinobu, and R. Donofrio. 2003. The Shiva crater: implications for Deccan volcanism, India-Seychelles rifting, dinosaur extinction, and petroleum entrapment at the KT boundary. GSA Abstracts with Programs 35:168.

Chatterjee, S. and N. Guven. 2002. The Shiva geophysical structure: another possible KT boundary impact crater on the western shelf of India. Abstract, 8th International Symposium on Mesozoic Terrestrial Ecosystems, Cape Town, South Africa, p. 36.

Chatterjee, S., and D. K. Rudra. 1996. KT events in India: impact, volcanism and dinosaur extinction. Memoirs of the Queensland Museum 39:489-532.

Chatterjee, S., and C. R. Scotese. 1999. The breakup of Gondwana and the evolution and biogeography of the Indian plate. Proceedings of Indian National Science Academy 65A:397-425.

Clube, S. V. M., and W. M. Napier. 1982. The role of episodic bombardment in geophysics. Earth and Planetary Science Letters 57:251-62.

Coffin, M. F., and W. M. Rabinowitz. 1982. Neogene sedimentary processes on the East African continental margin. EOS (American Geophysical Union Transactions) 63:445-446.

Courtillot, V. 1990. A volcanic eruption. Scientific American 263:85-92.

Courtillot, V., G. Feraud, H. Maluski, D. Vandamme, M. G. Moreau, and J. Besse. 1988. Deccan flood basalts and the Cretaceous/Tertiary boundary. Nature 333:843-846.

Courtillot, V., Y. Gallet, R. Rocchia, G. Feraud, E. Robin, C. Hoffman, N. Bhandari, and Z. G. Ghevariya. 2000. Cosmic markers, $^{40}Ar/^{39}Ar$ dating and paleomagnetism of the KT sections in the Anjar area of the Deccan large igneous province. Earth and Planetary Science Letters 182:137-156.

De, A. 1981. Late Mesozoic-Lower Tertiary magma types of Kutch and Saurasthra. Geological Society of India Memoir 3:327-339.

Donofrio, R. R. 1981. Impact craters: implications for basement hydrocarbon production. Journal of Petroleum Geology 3:279-302.

Donofrio, R. R. 1998. North American impact structures hold giant field potential. Oil and Gas Journal 96:69-83.

Duncan, R. A., and D. G. Pyle. 1988. Rapid eruption of the Deccan flood basalts at the Cretaceous/Tertiary boundary. Nature 33:841-843.

Dyment, J. 1998. Evolution of the Carlsberg Ridge between 60 and 45 Ma: ridge propagation, spreading asymmetry, and the Deccan-Reunion hotspot. Journal of Geophysical Research 103:24,067-24,084.

Ellwood, B. B., W. D. MacDonald, C. Wheeler, and S. L. Benoist. 2003. The K-T boundary in Oman: identified using magnetic susceptibility field instruments with geochemical confirmation. Earth and Planetary Science Letters 206:529-540.

Elkins-Tanton, L. T., and B. H. Hager. 2005. Giant meteoroid impacts can cause volcanism. Earth and Planetary Science Letters 239:219-232.

Fiske, P. S., W. J. Nellis, M. Lipp, H. Lorenzana, M. Kikuchi, and Y. Syono. 1955. Pseudotachylites generated in shock experiments: implications for impact cratering products and processes. Science 270:281-283.

Frankel, C. 1999. The end of the dinosaurs. Cambridge University Press, Cambridge, United Kingdom.

Gault, D. E., and P. Wedekind. 1978. Experimental studies of oblique impact. Proceedings of the Lunar and Planetary Science Conference 9:3843-3875. Pergamon Press, New York, New York.

Glen, W. 1990. What killed the dinosaurs? American Scientist 78:354-370.

Glen, W. 1994. The mass extinction debates: how science works in a crisis. Stanford University Press, Stanford, California.

Grajales-Nishimura, J. M., E Cedillo-Pardo, C. Rosales-Dominguez, D. Morian-Zenteno, W. Alvarez, P. Claeys, J. Ruiz-Morales, P. Padilla-Avilla, and A. Sanchez-Rios. 2000. Chicxulub impact: the origin of reservoir and seal facies in the southeastern Mexico oil fields. Geology 28:307-310.

Grieve, R. A. F. 1987. Terrestrial impact structures. Annual Review of Earth and Planetary Sciences 15:245-270.

Grieve, R. A. F. 1990. Impact cratering on Earth. Scientific American 261:66-73.

Grieve, R. A. F. 1998. Extraterrestrial impact on Earth: the evidence and the consequences. Geological Society of London Special Publications 140:105-131.

Grieve, R. A. F., and M. J. Cintala. 1992. An analysis of differential impact melt-crater scaling and implications for the terrestrial impact record. Meteoritics 27:526-538.

Hartnady, C. J. H. 1986. Amirante basin, western Indian Ocean: possible impact site at the Cretaceous-Tertiary extinction bolide? Geology 14:23-426.

Heymann, D., L. P. F. Chibante, P. R. Brooks, W. S. Wolbach, and R. E. Smalley. 1994. Fullerenes in the K/T boundary layer. Science 265:645-647.

Hildebrand, A. R., G. T. Penfield, D. A. King, M. Pilkington, A. Z. Camaro, S. B. Jacobson, and W. B. Boynton. 1991. Chicxulub Crater: a possible Cretaceous/Tertiary boundary impact crater on the Yucatan Peninsula, Mexico. Geology 19:867-871.

Hildebrand, A. R., M. Pilkington, M. Connors, C. Ortiz-Aleman, and R. E. Chavez. 1995. Size and structure of the Chicxulub Crater revealed by horizontal gravity gradients and cenotes. Nature 376:415-417.

Hofmann, C., G. Feraud, and V. Courtillot. 2000. ^{40}Ar/^{39}Ar dating of mineral separates and whole rock from the Western Ghats lava pile: further constraints on duration and age of the Deccan Traps. Earth and Planetary Science Letters 180:13-27.

Hörz, F. 1982. Ejecta of the Ries Crater, Germany. Geological Society of America Special Paper 190:39-55.

Hörz, F., T. H. See, A. V. Murali, and D. P. Blanchard. 1989. Heterogeneous dissemination of projectile materials in the impact melts from Wabar crater, Saudi Arabia. Proceedings of the Lunar and Planetary Science Conference 19:696-709.

Howard, K. A., and H. G. Wilshire. 1975. Flows of impact melt at lunar craters. Journal of Research, U. S. Geological Survey 3:237-251.

Izett, G. 1990. The Cretaceous/Tertiary boundary interval, Raton Basin, Colorado and New Mexico. Geological Society of America Special Paper 249:1-100.

Johnson, D. A., W. A. Berggren, and J. E. Damuth. 1982. Cretaceous ocean floor in the Amirante Passage: tectonics and oceanographic implications. Marine Geology 47:331-343.

Jones, A. P., G. D. Price, N. J. Price, P. S. DeCarli, and R. A. Clegg. 2002. Impact induced melting and the development of large igneous provinces. Earth and Planetary Science Letters 202:551-561.

Kaila, K. L., P. R. K. Murty, V. K. Rao, and G. E. Kharetchko. 1981. Crustal structure from deep-seismic surroundings along the Koyna II (Kelsi-Loni) profile in the Deccan trap area, India. Tectonophysics 73:365-384.

Kastner, M., F. Asaro, H. V. Michel, W. Alvarez, and L. W. Alvarez. 1984. Did the clay minerals at the Cretaceous-Tertiary boundary form from the glass? Evidence from Denmark and DSDP hole 465A. Journal of Non-crystalline Solids 67:463-464.

Keller, G., T. Adatte, W. Stinnesbeck, M. Rebolledo-Vieyra, J. U. Fucugauchi, U. Kramer, and D. Stüben. 2004. Chicxulub impact predates the K-T boundary mass extinction. Proceedings of the National Academy of Sciences 101:3753-3768.

Keller, G., W. Stinnesbeck, T. Adatte, and D. Stueben. 2003. Multiple impacts across the Cretaceous-Tertiary boundary. Earth-Science Reviews 62:327-363.

Kelley, P. S., and E. Gurov. 2002. Boltysh, another end-Cretaceous impact. Meteoritics and Planetary Science 37:1031-1043.

Koeberl, C., and R. R. Anderson. 1996. Manson and company: impact structures in the United States. Geological Society of America Special Paper 302:1-29.

Kyte, F. T., and J. A. Bostwick. 1995. Magnesioferrite spinel in Cretaceous/Tertiary boundary sediments of the pacific basin: remnants of hot, early ejecta from the Chicxulub impact? Earth and Planetary Science Letters 132:113-127.

Lightfoot, P. C., C. J. Hawkesworth, and S. F. Sethna. 1987. Petrogenesis of rhyolites and trachytes from the Deccan trap: Sr, Nd and Pb isotope and trace element evidence. Contribution to Mineralogy and Petrology 95:44-54.

Madahavraju, J., H. J. Hansen, S. Ramasamy, and S. P. Mohan. 2003. Magnetic susceptibility of Late Maastrichtian sediments of Ariyalur Group of Tiruchirapalli Cretaceous, Tamil Nadu. Journal of the Geological Society of India 61:699-702.

Mahadevan, T. M. 1994. Deep continental structure of India: a review. Geological Society of India Memoir 28:1-562.

Mahoney, J. J. 1988. Deccan Traps. Pp. 151-194 in Continental flood basalts (J. D. Macdougall, ed.). Kluwer Academic Publishers, Dordrecht, Netherlands.

Mahoney, J. J., R. A. Duncan, W. Khan, E. Gnos, and G. R. McCormick. 2002. Cretaceous volcanic rocks of the South Tethyan suture zone, Pakistan: implications for the Reunion hotspot and Deccan Traps. Earth and Planetary Science Letters 203:295-310.

Mart, Y. 1988. The tectonic setting of the Seychelles, Mascarene and Amirante plateaus in the western equatorial Indian Ocean. Marine Geology 79:261-274.

Mathur, R. B., and K. M. Nair. 1993. Exploration of Bombay Offshore Basin. Pp 365-396 in Proceedings of the second symposium on petroliferous basins of India (S. K. Biswas, ed.). Indian Petroleum Publishers, Dehra Dun, India.

McKenzie, D. P., and R. S. White. 1989. Volcanism at rifts. Scientific American 261:62-71.

McNulty, B. A. 1995. Pseudotachylite generated in the semi-brittle and brittle regimes, Bench canyon shear zone, central Sierra Nevada. Journal of Structural Geology 17:1507-1521.

Mehrotra, N. C., S. N. Swamy, and R. S. Rawat. 2001. Reworked Carboniferous palynofossils from Panna Formation, Bombay Offshore basin: clue to hidden target for hydrocarbon exploration. Journal of the Geological Society of India 57:239-248.

Melosh, H. J. 1989. Impact cratering: a geologic process. Oxford University Press, New York, New York.

Morgan, W. J. 1981. Hotspot tracks and the opening of the Atlantic and Indian Oceans. Pp. 443-487 in The sea (C. Emiliani, ed.). Wiley, New York, New York.

Moore, H. J. 1976. Missile impact craters (White Sands Missile Range, New Mexico) and applications to lunar research. Geological Survey Professional Papers 812B: B1-B47.

Negi, J. G., O. P. Pandey, and P. K. Agarwal. 1986. Super mobility of hot Indian lithosphere. Tectonophysics 131:147-156.

Negi, J. G., P. K. Agarwal, O. P. Pandey, and A. P. Singh. 1993. A possible K-T boundary bolide impact site offshore near Bombay and triggering rapid Deccan volcanism. Physics of the Earth and Planetary Interiors 76:189-197.

Officer, C. B., A. Hallam, C. L. Drake, J. D. Devine, and A. A. Meyerhoff. 1987. Late Cretaceous paroxysmal Cretaceous/Tertiary extinctions. Nature 326:143-149.

Pande, K, T. R. Venkatesan, K. Gopalan, P. Krishnamurthy, and J. D. McDougall. 1988. $^{40}Ar/^{39}Ar$ ages of alkali basalts from Kutch, Deccan volcanic provinces of India. Geological Society of India Memoir 10:145-150.

Pandey, J. 1990. Cretaceous/Tertiary boundary, iridium anomaly and foraminiferal breaks in the Um Sohryngkew river section, Meghalaya. Current Sciences 59:570-575.

Pandey, O. P., P. J. Agarwal, and J. G. Negi. 1996. Evidence of low density subcrustal underpinning beneath western continental region of India and adjacent Arabian Sea: geodynamical considerations. Journal of Geodynamics 21:365-377.

Pandey, O. P., and P. K. Agarwal. 2001. Nature of lithosphere deformation beneath the western continental margin of India. Journal of the Geological Society of India 57:497-505.

Parthasarathy, G., N. Bhandari, M. Vairamani, A. C. Kunwar, and B. Narasaiah. 2002. Natural fullerenes from the Cretaceous-Tertiary boundary later at Anjar, Kutch, India. Geological Society of America Special Paper 356:345-350.

Patriat, P., and J. Achache. 1984. India-Eurasia collision chronology has implications for crustal shortening and driving mechanism of plates. Nature 311:615-621.

Paul, D. K., P. J. Potts, D. C. Rex, and R. D. Beckingsale. 1977. Geochemical and petrogenetic study of the Girnar igneous complex, Deccan volcanic province, India. Geological Society of America Bulletin 88:227-234.

Pilkington, M., and R. A. F. Grieve. 1992. The geophysical signatures of terrestrial impact craters. Reviews of Geophysics 10:161-181.

Rao, R. P., and S. N. Talukdar. 1980. Petroleum geology of Bombay High field, India. American Association of Petroleum Geologists Memoir 30:487-506.

Ramalingeswara Rao, B. 2000. Historical seismicity and deformation rates in the Indian peninsular shield. Journal of Seismology 4:247-258.

Reimold, W. U. 1995. Pseudotachylite in impact structures-generation by fraction melting and shock brecciation? A review and discussion. Earth Science Reviews 39:247-265.

Robertson, D. S., M. Mckenna, O. B. Toon, S. Hope, and J. A. Lillegraven. 2004. Survival in the first hours of the Cenozoic. Geological Society of America Bulletin 116:760-763.

Robin, E., P. Bonte, L. Froget, C. Jehanno, and R. Rocchia. 1992. Formation of spinels in cosmic objects during atmospheric entry: a clue to the Cretaceous-Tertiary boundary event. Earth and Planetary Science Letters 108:181-190.

Robin, E., R. Rocchia, N. Bhandari, and P. N. Shukla. In press. Cosmic imprints in the Meghalaya K/T section. Journal of Earth System Science.

Sahni, A., B. S. Venkatachala, R. K. Kar, A. Rajaknath, T. Prakash, G. V. R. Prasad, and R. Y. Singh. 1996. New palynological data from the Deccan intertrappean beds: implications for the latest record of dinosaurs and synchronous initiation of volcanic activity in India. Geological Society of India Memoir 37:267-283.

Schaef, H. T. 1991. Cretaceous-Tertiary Clays in Central India. M.S. Thesis, Texas Tech University, Lubbock, Texas.

Schultz, P. H., and S. L. D'Hondt. 1996. Cretaceous-Tertiary (Chicxulub) impact angle and its consequences. Geology 24:963-967.

Schultz, P. H., and D. E. Gault. 1990. Prolonged global catastrophes from oblique impacts. Geological Society of America Special Paper 247:239-261.

Schultz, P. H., and R. E. Lianza. 1992. Recent grazing impacts on the Earth recorded in the Rio Cuarto Crater field, Argentina. Nature 355:234-237.

Scotese, C. R. 1997. Paleogeographic Atlas. PALEOMAP Project, University of Texas, Arlington, Texas.

Sen, G. 1988. Possible depth of origin of primary Deccan tholeiitic magma. Geological Society of India Memoir 10:25-51.

Sethna, S. F. 1989. Petrology and geochemistry of the acid, intermediate and alkaline rocks associated with the Deccan basalts in Gujrat and Maharashtra. Geological Society of India Memoirs 15:47-61.

Sheth, H. C. 1998. A reappraisal of the coastal Panvel flexure, Deccan Traps, as a listric-fault controlled reverse drag structure. Tectonophysics 294:143-149.

Sheth, H. C., and J. S. Ray. 2002. $Rb/Sr^{87}-Sr^{86}$ variations in Bombay trachytes and rhyolites (Deccan Traps): Rb-Sr isochron, or AFC process? International Geology Review 44:624-638.

Shukla, A. D., N. Bhandari, S. Kusumgar, P. N. Shukla, Z. G. Ghevariya, K. Gopalan, and V. Balaram. 2001. Geochemistry and magnetostratigraphy of Deccan flows at Anjar, Kutch. Proceedings Indian Academy of Sciences 110:111-132.

Sisodia, M. S., U. K. Singh, G. Lakshari, P. N. Shukla, A. D. Shukla, and N. Bhandari. 2005. Mineralogy and trace element chemistry of the Siliceous Earth of Barmer Basin, Rajasthan: evidence for a volcanic origin. Journal of Earth System Science 114:111-124.

Smit, J. 1999. The global stratigraphy of the Cretaceous-Tertiary boundary impact ejecta. Annual Review of Earth and Planetary Sciences 27:75-113.

Smit, J., and G. Klaver. 1981. Sanidine spherules at the Cretaceous-Tertiary boundary indicate a large impact event. Nature 292:47-49.

Srivastava, A. K. 1996. Determination of satellite gravity from closely spaced repeat passes of ERS-1 altimeter and preparation of gravity maps for the Indian offshore and adjoining area. Pp. 22 in Annual Report of Keshava Deva Malaviya Institute of Petroleum Exploration, Dehra Dun, India.

Stewart, S. A., and J. P. Allen. 2002. A 20-km-diameter multi-ringed impact structure in the North Sea. Nature 418:520-523.

Sutherland, F. L. 1996. The Cretaceous/Tertiary-boundary impact and its global effects with reference to Australia. Journal of Australian Geology and Geophysics 16:567-585.

Swisher, C. C., J. M. Grajales-Nishimura, A. Montanari, S. V. Margolis, P. Clayes, W. Alvarez, P. Renne, E. Cedillo Pardo, F. J.-M. R. Maurasse, G. H. Curtis, J. Smit, and M. O. McWilliams. 1992. Coeval $^{40}Ar/^{39}Ar$ ages of 65.0 million years ago from Chicxulub Crater melt rock and Cretaceous-Tertiary boundary tektites. Science 257:954-958.

Talwani, M., and C. Reif. 1998. Laxmi Ridge – a continental sliver in the Arabian Sea. Marine Geophysical Research 20:259-271.

Toon, O. B., K. Zahnle, D. Morrison, R. P. Turco, and C. Covey. 1997. Environmental perturbations caused by the impacts of asteroids and comets. Reviews of Geophysics 35:41-78.

Underhill, J. R. 2004. An alternative origin for the 'Silverpit crater.' Nature 428(6980):1-2.

Venkatesan T. R. 1990 Ar-Ar studies of Malani complex in Rajasthan, India: evidences for different magmatic episodes. Journal of the Geological Society of Australia 27:106.

Wandrey, C. J. 2004. Bombay Geologic Province Eocene to Miocene Composite Total Petroleum System, India. U. S. Geological Survey Bulletin 2208-F:1-20.

Wetherill, G. W., and G. M. Shoemaker. 1982. Collision of astronomically observable bodies with the Earth. Geological Society of America Special Paper 190:1-13.

White, R. S., and D. P. McKenzie. 1989. Volcanism at rifts. Scientific American 261:62-71.

White, R. V., and A. D. Saunders. 2005. Volcanism, impact and mass extinctions: incredible or credible coincidences? Lithos 79:299-316.

Wilhelms, D. E. 1987. The geologic history of the Moon. U. S. Geological Survey Professional Paper 1348:1-302.

Yurk, Y. Y., G. K. Yeremenko, and Y. A. Polkanov. 1975. Boltyshskaya kotlovinaiskopayemyy meteoritnyy krater. Sovetskaya Geologiya 2:38-144.

Zutshi, P. L., A. Sood, P. Mohapatra, K. K. V. Raman, A. K. Dwivedi, and H. C. Srivastava. 1993. Lithostratigraphy of Indian petroliferous basins, Documents V. Bombay Offshore Basin, Unpublished KDMIPE Report, ONGC, Dehra Dun, India.

Addresses of Authors:

SANKAR CHATTERJEE

Department of Geosciences
Museum of Texas Tech University
MS/Box 43109
Lubbock, TX 79409
sankar.chatterjee@ttu.edu

NECIP GUVEN

Department of Geosciences
Texas Tech University
MS/Box 1053
Lubbock, TX 79409
necip.guven@ttu.edu

AARON YOSHINOBU

Department of Geosciences
Texas Tech University
MS/Box 1053
Lubbock, TX 79409
aaron.yoshinobu@ttu.edu

RICHARD DONOFRIO

Exploration and Development Geosciences
University of Oklahoma
Norman, OK 73069
Parwest512@aol.com